

Characterization of nitrous acid and its potential effects on secondary pollution in warm-season of Beijing urban areas

Junling Li¹, Chaofan Lian^{2, #}, Mingyuan Liu³, Hao Zhang¹, Yongxin Yan¹, Yufei Song¹, Chun Chen¹, Jiaqi Wang¹, Haijie Zhang¹, Yanqin Ren¹, Yucong Guo², Weigang Wang², Yisheng Xu¹, Hong Li^{1, *}, Jian Gao^{1, *}, Maofa Ge^{2, *}

- 5 ¹ State Key Laboratory of Environmental Criteria and Risk Assessment, Chinese Research Academy of Environmental Sciences, Beijing 100012, China
² State Key Laboratory for Structural Chemistry of Unstable and Stable Species, Beijing National Laboratory for Molecular Sciences (BNLMS), CAS Research/Education Center for Excellence in Molecular Sciences, Institute of Chemistry, Chinese Academy of Sciences, Beijing 100190, China
³ China National Environmental Monitoring Centre, Beijing, 100012, China
Now at Assessment and Research Center for Pollution and Carbon Reduction, Tianfu Yongxing Laboratory, Chengdu 610213, China
- 10 *Correspondence to:* Hong Li (lihong@craes.org.cn), Jian Gao (gaojian@craes.org.cn), Maofa Ge (gemaofa@iccas.ac.cn)

Abstract. As a key source of hydroxyl (OH) radical, nitrous acid (HONO) has attracted much attention for its important role in the atmospheric oxidant capacity (AOC) increase. In this study, we made a comparative study on the ambient levels, variation patterns, sources, and formation pathway in warm season (from June to October in 2021) on a basis of a continuous intensive observation in an urban site of Beijing. The monthly average mixing ratio of HONO were 1.3 ppb, 1.3 ppb, 1.0 ppb, 15 0.96 ppb, 0.89 ppb, respectively, showing a larger contribution to OH radical relative to ozone at daytime. The emission factor (EF) relative to NO_x from the vehicle emissions, was estimated to be 0.017, higher than most studies conducted in Beijing. The average nocturnal NO₂ to HONO conversion frequency k_{HONO} were 0.008 h⁻¹. In warm seasons, the missing source of HONO, P_{unknown} , around noontime were 0.29-2.7 ppb/h. According to the OH production from HONO, the OH production rate from the missing HONO was also very important to atmospheric oxidation capacity (AOC). This work 20 highlights the importance of HONO for AOC in warm season, while encouraging long-term HONO observation to assess the contribution of HONO sources over time compared to the capture of pollution processes.

1 Introduction

From 2013 to 2022, the annual average concentration of PM_{2.5} in China has been decreasing, but it is still much higher than the World Health Organization's guideline value (5 μg/m³). Ozone pollution, on the other hand, is becoming more and 25 more prominent (Liu et al., 2023b; Li et al., 2022). China's air quality problem has developed from being dominated by PM_{2.5} in the past to being affected by the photochemical pollutants PM_{2.5} and ozone, that is, “Air Pollution Complex” (Zhu et al., 2023). The atmospheric oxidation capacity (AOC) determines the production rates of secondary pollutants in the atmosphere, and is the essential driving force in forming complex air pollution (Liu et al., 2021b).

As a trace gaseous pollutant, nitrous acid (HONO) strongly impacts the AOC, the photolysis of which can contribute to 30 more than 60% of the OH radicals at daytime (Czader et al., 2012). As an important source of OH radicals in both rural and urban environments, HONO outweighs the contribution of ozone photolysis (Gu et al., 2022; Elshorbany et al., 2012; Yang et

al., 2021b). Thus, as an important source of oxidants for AOC, HONO can substantially influence the formation of secondary pollutants, exerting a considerable impact on air quality, climate change, and human health (Requia et al., 2018;Zhang et al., 2021b;Huang et al., 2018;Liu et al., 2023b).

35 Due to the importance of HONO to AOC, researchers have done lots of work on the transformation process of HONO, i.e., source and sink. For the source of HONO, it is complicated and has been debated for decades. To sum it up, source of atmospheric HONO mainly includes: (a) direct emission from combustion, soil, and livestock farming. The combustion includes vehicle exhaust, industrial exhaust, and biomass burning (Liao et al., 2021;Kurtenbach et al., 2001;Kirchstetter et al., 1996;Nie et al., 2015). The release from soil nitrite is one important primary source of HONO (Su et al., 2011; VandenBoer
40 et al., 2015; Wu et al., 2019), the biological soil crusts can accelerate the HONO emission in drylands (Weber et al., 2015), fertilization behavior of agricultural fields remarkably enhance the emission of HONO (Xue et al., 2021), and denitrification is one major HONO production pathway in boreal agricultural fields (Bhattarai et al., 2021). Meanwhile, livestock farming is also identified as one important primary emission source of HONO (Zhang et al., 2023a). (b) Homogeneous reaction of OH +NO. This is an important source of HONO. Although the reaction of OH+NO, which is the reverse reaction of HONO
45 photolysis, does not contribute to an actual increase in free radicals, the assessment of this reaction pathway is significant for understanding the sources and sinks of HONO. Especially during the winter pollution period in North China Plain, where there is usually a higher concentration of NO, this reaction pathway will contribute to a higher concentration of HONO (Xue et al., 2020). (c) Heterogeneous conversion of NO₂ on various surfaces (Liu et al., 2023a;Yu et al., 2022a;Yang et al., 2021a), Finlayson-Pitts et al. (2003) reported that NO₂ could be converted to HONO on humid surfaces with first order in NO₂, Xu et
50 al. (2015) highlighted the HONO source had a large variability with heterogeneous conversion of NO₂ at ground face, Aubin and Abbatt (2007) found that the heterogeneous conversion of NO₂ on hydrocarbon surfaces was an effective pathway to generate HONO. (d) photolysis of nitric acid and nitrate in particles at daytime, which were considered as important sources of HONO in both experiments and field observations (Wang et al., 2023b;Ye et al., 2019;Yang et al., 2018;Ye et al., 2017). And for the sinks of HONO, diurnal photolysis is the main consumption way (Keller-Rudek et al., 2013), the reaction of
55 HONO with OH radical is also one sink that needs to be paid attention to (Cox et al., 1976).

Generally, HONO concentration in the atmosphere is closely related to the quality of the atmosphere. As the heterogeneous processes are considered as the main source of HONO, and most of which are poorly understood, therefore, many field observations of HONO were focus on haze polluted environments (Li et al., 2012;Spataro et al., 2013;Tong et al., 2015;Xu et al., 2015;Hou et al., 2016). In urban areas, the HONO concentration can be up to more than 10 ppb during severe
60 pollution episode (Zhang et al., 2019b). In China, the Chinese government has implemented series of stringent clean air actions to address the severe air pollution issue since 2013, significant reduction of PM_{2.5} was observed in North and South China during 2013-2020 (Li et al., 2022). However, ozone levels have not been effectively reduced in China, the warm-season (from April to September) mean maximum daily 8 h average ozone (MDA8 O₃) increased by 2.6 μg/(m³·yr) (Liu et al., 2023b). In view of the atmospheric changes in PM_{2.5} and ozone, recent field observations have begun to pay attention to
65 the potential influence of HONO on PM_{2.5}, ozone, and coexistence of PM_{2.5} and ozone (Zhang et al., 2023c;Zhang et al.,

2023b;Xuan et al., 2023;Chen et al., 2023;Zhang et al., 2022;Lin et al., 2022;Li et al., 2021). However, most HONO observations were conducted in autumn and winter, and the period were relatively short, usually a few weeks covering one or several pollution processes. Based on the increase of ozone in warm-season, long-term observations during the warm season are needed, yet is rather limited.

70 In this work, we conducted one HONO observation in an urban site of Beijing, the time was from June to October 2021, covering the whole summer and part of autumn. According to the Technical Regulation on Ambient Air Quality Index in China, only one day of moderate pollution (PM_{2.5}, in October) and no more than four days of light pollution (ozone) per month were included, so we analysed the observation data on a monthly basis. The atmospheric levels and variations of HONO and related species during each month were analysed and compared. The impacts of HONO on atmospheric oxidant
75 capacity in each month were also assessed.

2 Methods

2.1 Observation site and instruments

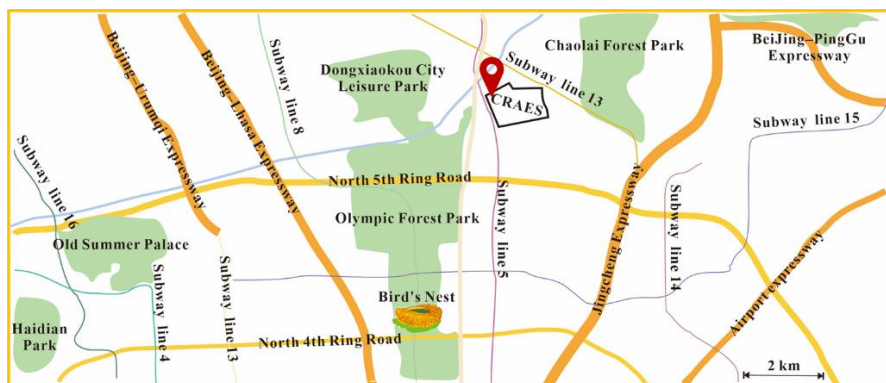


Figure 1: Location of the observation site in this work.

80 The observation campaign was conducted from June 18th, 2021 to October 25th, 2021. The observation site was located at Chinese Research Academy of Environmental Sciences (CRAES, 40°04'N, 116°42'E), in the north of Chaoyang District, an urban site (Ren et al., 2022;Zhang et al., 2021a) in Beijing, China (Figure 1). Briefly, Chaoyang District was located at the eastern area of Beijing and was one of the six main urban districts (Dongcheng, Xicheng, Haidian, Chaoyang, Shijingshan, and Fengtai) of Beijing. This site was located about 2 km to the north of the North Fifth Road, approximately 0.3 km away
85 from Beiyuan Road, with a high volume of traffic. And this site was located in a mixed-use commercial and residential area, with several shopping malls, residential areas, and office buildings nearby, and there were no obvious sources of industrial pollution. Thus, this site could be considered as an urban site.

HONO was measured with a water-based long-path absorption photometer (Chen et al., 2020), the potential interferences, e.g., hydrolysis of NO₂, was subtracted by deployed a dual-channel absorption system. Briefly, the main

90 structure of the instrument sampling unit is a double-channel stripping coil. In the first coil, almost all of the HONO and a
small fraction of interfering species (e.g., NO₂, peroxyacetyl nitrate, NO₂⁻) are absorbed by deionized water; while in the
second channel, only a small fraction of interfering species is absorbed, which could be seen as the comparable conversion
ratio in both the first and second channels. Therefore, the HONO concentration output by the instrument is the difference in
concentration between the first and second channels. As to the soluble species such as HO₂NO₂, considering its little ambient
95 concentration, especially in warm season, the interfering could be neglected. A set of commercial analysers (Thermo 42i, 43i,
48i, 49i, 5030i, USA) were used to measure the concentrations of NO_x, SO₂, CO, O₃, and PM_{2.5} online. Due to the
employment of a molybdenum NO₂-to-NO converter, the 42i analyzer might overestimate NO₂ concentration for the
potential conversion of NO_z (NO_z = NO_y - NO_x. e.g., HONO, HNO₃, peroxyacetyl nitrate (PAN), and so on). Based on this,
we conducted field observations of NO₂ from May 19th to 31st, 2024, using two devices with different measurement
100 principles (Figure S1). The observation results showed that when the NO₂ concentration was above 7 ppb, there was no
significant difference between the two devices. However, when it was below 7 ppb, the 42i values were significantly higher
than those of the N500, with a corresponding slope of 1.14. Based on this data, we have adjusted all NO₂ values below 7 ppb
during the observation period, as well as the corresponding analyses. The time resolution of the analysers above were 1min,
and the detection limits were 0.4 ppbv, 0.5 ppbv, 0.04 ppmv, 1ppbv, and 0.5 µg/m³, respectively. In order to ensure the
105 accuracy of the data, routine maintenance was carried out. The meteorological parameters (temperature, T; relative humidity,
RH; pressure, P; wind speed and direction, WS and WD) were obtained with an automatic weather station (MAWS301,
Vaisala, Finland) with a time resolution of 1 hr. Mass concentrations of the inorganic compositions in PM_{2.5} (NO₃⁻, SO₄²⁻, Cl⁻)
were detected with a Monitor for AeRosols and Gases in ambient Air (MARGA, Model ADI 2080, Applikon Analytical
B.V., the Netherlands) with 1 hr resolution. Detailed descriptions of the instrument inlet design and the operating
110 characteristics can be referred in previous studies (Wang et al., 2022).

2.2 Photolysis rate simulation and OH estimation

Photolysis frequencies of JNO₂ were measured by a filter radiometer (METCON, Germany) with a time resolution of 1 min.
Photolysis rate constant of O₃, HONO, and other parameters were simulated according to the aerosol optical depth and solar
zenith angle by the weather research and forecasting model coupled with chemistry (WRF-Chem, version 3.7.1), based on
115 the TUV model (<http://cprm.acom.ucar.edu/Models/TUV/InteractiveTUV/>) (Zhang et al., 2019a). To reduce the imprecision
of model simulation, the observed JNO₂ value was used to correct simulated results, i.e., J(O¹D) and J(HONO).

The OH concentration was calculated with the following equation (Liu et al., 2019):

$$[OH] = a \times \left(\frac{J(O^1D)}{10^{-5} s^{-1}} \right)^b + c \quad (1)$$

where $a = 4.2 \times 10^6 \text{ cm}^{-3}$, $b = 1$, $c = 2.2 \times 10^5 \text{ cm}^{-3}$ (Lin et al., 2022), these coefficients adopted here were from the OH
120 studies in the Pearl River delta (PRD) and Beijing, China (Rohrer et al., 2014; Tan et al., 2017, 2018). The influence of the
uncertainty of the coefficients was estimated (Liu et al., 2019), results showed that the errors of OH increased with the

increase of $J(O^1D)$, but the ratios of error to mean value of OH radicals were in an acceptable range of 0.37-0.55. According to the summarizing coefficients in different OH observation campaigns in the polluted areas of China (Liu et al., 2019), the comprehensive impact of reactants (e.g., VOCs and NO_x) on OH could not compete with that of UV light to OH, the chemical environments of OH could be similar. The OH concentration calculated through this formula was within a reasonable range and would not subvert the relative conclusions in this study. Thus, this could be a reasonable way to derive OH concentration by the equation above.

3 Results and discussion

3.1 Observation data overview

3.1.1 Variations of meteorological parameters during observation period

Figure S2 shows the time series of meteorological parameters including RH, T, WS, WD, and JNO_2 from June 18th, 2021 to October 25th, 2021. During the observations, the temperature ranged from 3.1-37 °C with an average of 23 °C, and the RH ranged from 7.1%-100% with an average of 59%. The average wind speed during the observation was 1.1 m/sec, and the maximum wind speed was 5.20 m/sec. The average and monthly average values of T, RH, and WS are shown in Table S1. As shown in Figure S3 and Table S1, the temperature in June, July, and August was higher, 26-29 °C, temperature began to drop slightly in September, 22 °C, in October, temperature dropped significantly, 13 °C. Meanwhile, the solar radiation in September and October decreased as the sun moved south. The maximum value of $J(NO_2)$ during the observation was $8.2 \times 10^{-3} s^{-1}$, the values reached a maximum at noon (with high solar radiation) and decreased to zero at night. The average wind speed also slightly decreased in September and October. During the observation, June had the lowest RH and the maximum wind speed; and due to the increase in precipitation, July had the highest RH. For the daily variation of meteorological parameters, T and JNO_2 expressed the same variation pattern with O₃, that was increasing after sunrise and decreasing after sunset, as shown in Figure S3. While the RH showed the opposite pattern that was increasing during night and decreasing during the daytime. For the WS, it was higher from 8 to 20 o'clock in June, and for the rest of the observation period, WS begun to increase in the afternoon and subside after sunset.

3.1.2 Variations of pollutant species during observation period

Figure 2 shows the time series of basic parameters including HONO, NO₂, NO, CO, O₃, SO₂, PM₁₀, PM_{2.5}, and HONO/NO₂ from June 18th, 2021 to October 25th, 2021. The HONO concentration ranged from 0.05 ppb to 5.2 ppb, with an averaged value of 1.1 ppb (the entire observation period). The concentration of O₃ ranged from 1ppb to 227 ppb, with an averaged value of 72 ppb (the entire observation period). The concentrations of NO₂, NO, CO, SO₂, and PM_{2.5} were 0.56-53 ppb, 0.01-210 ppb, 0.1-1.6 ppm, 1.3-4.6 ppb, and 1-181 $\mu g/m^3$, respectively, with average values (the entire observation period) of 10 ppb, 7.9 ppb, 0.56 ppm, 1.9 ppb, 19 $\mu g/m^3$, respectively. The average and monthly average concentrations of the basic

parameters are shown in Table 1. One haze episode (1 day) occurred across the observation period, the daily mass concentration of PM_{2.5} was 117 µg/m³, higher than the National Ambient Air Quality Standard (Class II: 75 µg/m³). And for O₃, eight episodes (13 days) occurred across the observation period, with MDA8 O₃ higher than the Class II: 160 µg/m³.
 155 Overall, the high HONO concentration was always accompanied by high concentration of NO_x (NO, NO₂) or aerosols (PM_{2.5}).

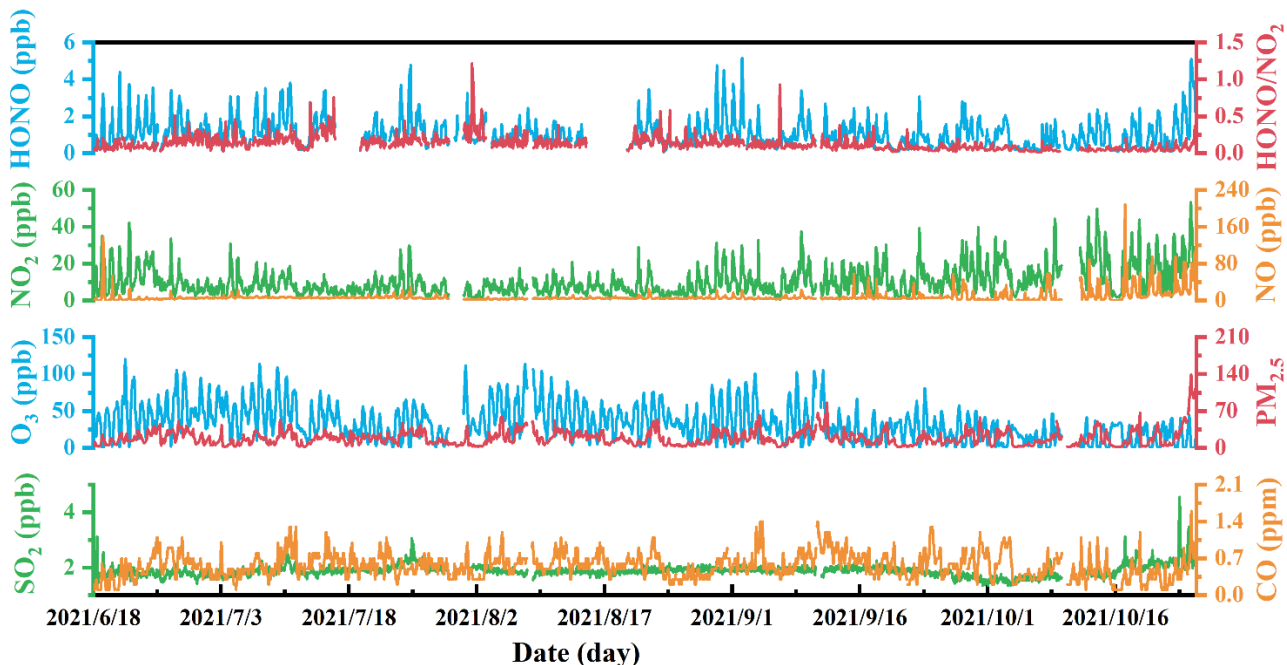


Figure 2: Temporal variations of hourly average PM_{2.5}, CO, O₃, SO₂, NO, HONO, NO₂, and HONO/NO₂ during the observation period.

160 Table 1. The average and monthly average concentration of HONO, NO₂, NO, CO, O₃, SO₂, PM_{2.5}, HONO/NO₂, and HONO/NO₂ from June to October during the observation period.

concentration		HONO (ppb)	NO ₂ (ppb)	HONO/NO ₂	NO (ppb)	CO (ppm)	O ₃ (ppb)	SO ₂ (ppb)	PM _{2.5} (µg/m ³)
average (the entire observation period)		1.1	10	0.052	7.9	0.56	72	1.9	19
Jun.	average	1.3	12	0.051	5.7	0.52	88	1.8	20
	max	4.4	42	0.17	139	1.1	227	4	51
	min	0.14	2	0.0055	0.3	0.1	1	1.4	3
Jul.	average	1.3	7.5	0.072	6.6	0.56	78	1.9	17
	max	4.8	31	0.54	29	1.3	211	3.1	53
	min	0.11	1.1	0.0061	2.2	0.1	1	1.5	1
Aug.	average	1.0	7.1	0.079	4.8	0.57	87	1.9	19
	max	4.8	31	0.79	24	1.2	214	2.2	60
	min	0.052	0.62	0.0049	1.3	0.2	10	1.5	2
Sep.	average	0.96	11	0.035	6.7	0.65	68	1.9	19

	max	5.2	40	0.19	57	1.4	210	2.3	86
	min	0.078	0.56	0.0042	0.39	0.2	9	1.3	1
Oct.	average	0.89	17	0.025	17	0.46	40	1.9	23
	max	5.1	53	0.21	210	1.6	116	4.6	181
	min	0.066	1.7	0.0041	0.01	0.1	10	1.3	1

3.2 HONO observation comparison and pollution patterns

3.2.1 HONO observation comparison

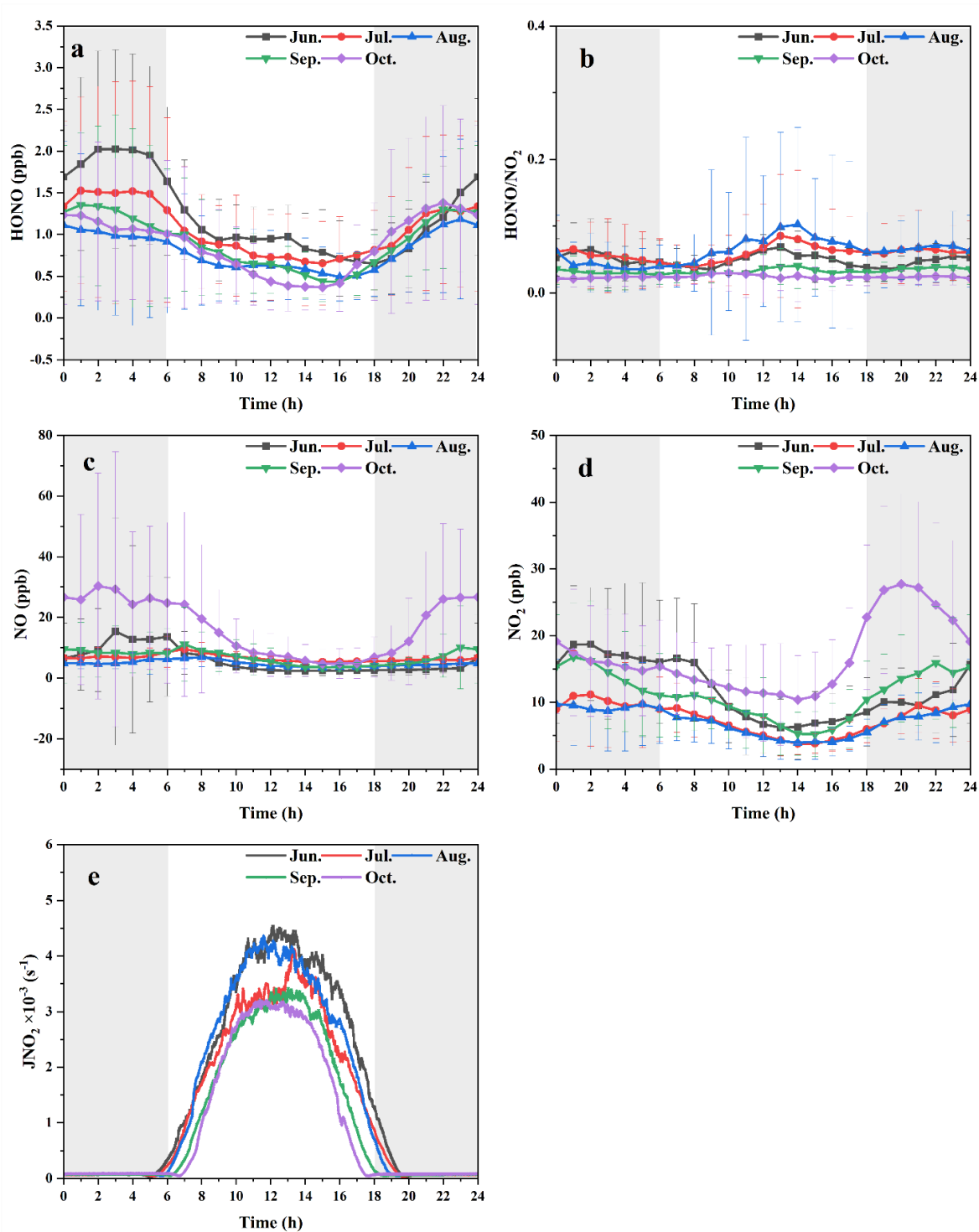
For comprehensive comparative analysis, a review of the HONO observations in Beijing was carried out in the past several years, and the results are shown in Table S2. Overall, the HONO measurement began to increase since 2016 in Beijing, the time was mainly concentrated in winter (Dec., Jan., and Feb.), and most of which were pollution process analyses. In this work, the observation period was in summer and autumn. When the air quality was relatively poor in early years, PM_{2.5} and HONO concentrations were both relatively high, now the air quality of Beijing was improved, both the concentration of PM_{2.5} and HONO decreased. However, during the observation period, PM_{2.5} concentration was low, HONO concentration was still relatively higher compared with other results performed in summer. According to previous studies (Murthy et al., 2020; Du et al., 2013), the narrowing of mixing layer could result in the accumulation of pollutants near the ground, while the increase of mixing layer height (MLH) favoured the dilution of pollutants. In general, the MLH was low in winter and high in summer. And the photochemistry was quite active in summer because of the strong solar radiation, in this case, HONO tended to undergo photolysis. However, our observations showed that HONO concentration in summer was comparable to that in winter and spring, and higher than that in autumn. Wang et al. (2023a) also found that in warm season, the PM_{2.5} and MDA8 O₃ increased along with the development of MLH (MLH < 1200 m), they analysed that the enhanced secondary chemical formation and increased atmospheric oxidant capacity could explain this phenomenon. Based on this, we discussed the HONO sources in the following sections.

3.2.2 HONO variation patterns

The average diurnal variation of the pollutants during the whole observation period and the averaged values in each month are shown in Figure S4 and Figure 3. It can be seen that the daily averaged pattern of pollutant HONO is that it decreased after sunrise and increased after sunset, this variation pattern was similar to previous studies (Lin et al., 2022; Lian et al., 2022; Zhang et al., 2019a; Zhang et al., 2023b; Zhang et al., 2022). This trend was the same as NO₂, NO, PM_{2.5}, and CO, that was, the overall was relatively stable, and it decreased slightly during the daytime. The diurnal variation of SO₂ was not large, and the overall concentration was very low, but it had a slightly increase during the daytime. The variation of O₃ showed the opposite trend, i.e., its concentration increased after sunrise, peaked in the afternoon and decreased at night. The rapid decrease of HONO in daytime was caused by rapid photolysis and the increase of boundary layer height. The ratio of HONO/NO₂ is often used to characterize the heterogeneous reaction of NO₂ to form HONO (Yang et al., 2021a; El Zein et al., 2013; Romanias et al., 2012). At night, the HONO/NO₂ ratio was similar to that of HONO, but the ratio increased

190 obviously during the daytime, especially in summer (Jun., Jul., Aug.), and in summer, the light intensity was very strong, as revealed in Figure 3b and 3e. This phenomenon indicated that HONO might have other potential sources related to the solar radiation, e.g., the conversation of NO_2 to HONO or nitrate photolysis.

And when HONO was analysed in months, the characteristics of each month were different. For the HONO/ NO_2 ratio in Figure 3b, August, July, June, and September were the months with a significant increase in the noon period, and there
195 was no such phenomenon in October. However, it was important to note that the NO and NO_2 concentration in October were the highest in the entire observation period compared to the low HONO concentration. The NO and NO_2 concentrations in June were not high, but the HONO concentration was the highest. The phenomenon could not be explained by the well-known sources of HONO (Xuan et al., 2023).



200 **Figure 3.** Diurnal variations in (a) HONO, (b) HONO/NO₂, (c) NO, (d) NO₂, and (e) JNO₂ in each month. The gray shading areas indicate nighttime, 18:00-06:00 LT.

3.3 Nocturnal HONO sources and formation

3.3.1 Direct emission of HONO

Previous studies showed that the primary emission sources of HONO included biomass burning and vehicles as well as soil emissions (Nie et al., 2015; Su et al., 2011). In this study, soil emission was a negligible source of HONO, since the observation site was located in an urban area, the surrounding soil was not used for agriculture, which greatly reduced HONO emission caused by fertilization process (Su et al., 2011). Except organic compounds (Simoneit, 2002), CO in the gas phase (Andreae, 2019) and potassium ions (K^+) in the aerosol phase (Xinghua et al., 2007) were well recognized inorganic tracers of biomass burning. Many CO sources other than biomass burning, such as industry and traffic, could contribute significantly to the CO loading. Apart from biomass burning emissions, there were no other significant sources of K^+ during the measurement. Therefore, K^+ was a suitable tracer of biomass burning. According to studies on the influence of biomass burning on HONO chemistry (Nie et al., 2015), when K^+ concentration is higher than $2 \mu\text{g m}^{-3}$ and the ratio of K^+ to $\text{PM}_{2.5}$ is larger than 0.02, the plumes are defined as biomass burning samples. While the samples with K^+ concentrations lower than $2 \mu\text{g m}^{-3}$ and a ratio of K^+ to $\text{PM}_{2.5}$ smaller than 0.02 are categorized as non-biomass burning samples. The average K^+ levels during the five months were 0.14, 0.11, 0.11, 0.15, and 0.13 $\mu\text{g/m}^3$, respectively, lower than $2 \mu\text{g/m}^3$ (Nie et al., 2015), which indicated that biomass burning had little effect on this observation site. Hence, only vehicle emission was considered in this study.

The HONO/ NO_x ratio was used to derive the emission factor of vehicles in fresh plumes (Kurtenbach et al., 2001). Criteria followed by the fresh plumes were (Yun et al., 2017):

- 220 (a) $\Delta\text{NO}/\Delta\text{NO}_x > 0.9$
- (b) good correlation between NO_x and HONO ($R^2 > 0.7$)
- (c) short duration of plumes < 1 h
- (d) positive correlation between CO and NO_x
- (e) no precipitation
- 225 (f) global radiation $< 10 \text{ W/m}^2$, or $J\text{NO}_2 < 0.25 \times 10^{-3} \text{ s}^{-1}$

A total of 6 cases met the criteria mentioned above and the details were summarized in Table 2. The mean $\Delta\text{NO}/\Delta\text{NO}_x$ ratio of the selected fresh plumes was $(97 \pm 4.4) \%$, which indicated that the chosen air masses were considered to be truly fresh. The linear slope of HONO with NO_x were used as the emission factors of HONO. The correlation coefficients (R^2) between HONO and NO_x varied among the cases due to the unavoidably mixing with other air masses, and the range was from 0.72 to 0.93. The obtained $\Delta\text{HONO}/\Delta\text{NO}_x$ ratios were from 0.32% to 2.49%, with an average value of $(1.7 \pm 0.74) \%$. Thus, a mean $\Delta\text{HONO}/\Delta\text{NO}_x$ value of 0.017 was used as the emission factor (EF) in this work. The $\Delta\text{HONO}/\Delta\text{NO}_x$ values obtained in urban area of Beijing in previous studies were also summarized in Table S2, the EF reported so far was concentrated in the range of 0.003-0.013, which was slightly lower than the EF in this work. The vehicle engine types,

catalytic converters use, and fuels could affect the emission factors of vehicles (Kurtenbach et al., 2001). According to
 235 Kessler and Platt (1984), diesel engines had a higher HONO/NO_x ratio than gasoline engines. In our study, the higher
 HONO/NO_x value possibly due to that the observation site was located outside the fifth ring road, and more heavy-duty
 diesel vehicles passed by on the surrounding road at night (regulations of the Public Security Traffic Management Bureau of
 the Beijing Municipal Public Security Bureau, i.e., from 6 a.m. to 11 p.m. every day, trucks are prohibited from passing on
 the roads within the Fifth Ring Road (exclusive), and trucks with an approved load weight of more than 8 tons (inclusive) are
 240 prohibited on the main road of the Fifth Ring Road). Assuming that NO_x mainly arose from vehicle emissions, the mean
 $\Delta\text{HONO}/\Delta\text{NO}_x$ value of 0.017 was adopted to estimate the vehicle emissions P_{emis} (ppb/h) contribution to the HONO
 concentration (this factor may lead to an overestimation of the P_{emis} at daytime):

$$P_{\text{emis}} = \text{NO}_x \times \text{EF} \quad (2)$$

Then the concentration of HONO in air that is not due to direct vehicular emissions (the corrected HONO concentration,
 245 $\text{HONO}_{\text{corr}}$) can be obtained from the following equation:

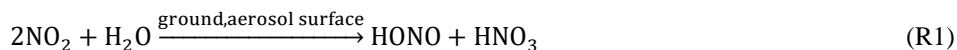
$$\text{HONO}_{\text{corr}} = \text{HONO} - P_{\text{emis}} \quad (3)$$

Table 2. Emission ratios ($\Delta\text{HONO}/\Delta\text{NO}_x$) of fresh vehicle plumes.

Date (yyyy/mm/dd)	Time	$\Delta\text{NO}/\Delta\text{NO}_x$		$\Delta\text{HONO}/\Delta\text{NO}_x$	
		Slope (%)	R ²	Slope (%)	R ²
2021/6/21	2:25-3:15	99	1	2.5	0.73
2021/8/31	2:20-2:45	93	0.99	2.2	0.76
2023/9/15	3:30-4:20	104	0.98	2.1	0.83
2023/9/22	5:20-5:50	96	0.97	2.0	0.85
2023/10/3	0:40-0:55	94	0.99	1.2	0.93
2023/10/8	4:35-5:25	94	0.99	0.32	0.79

3.3.2 Nighttime heterogeneous conversion of NO₂

Heterogeneous conversion of NO₂ on ground or aerosol surface has been recognized as an important HONO source
 250 (Finlayson-Pitts et al., 2003; Liu et al., 2020). Nighttime $\text{HONO}_{\text{het-night}}$ concentration could be estimated from the
 heterogeneous reaction (R1, the mechanism of heterogeneous formation of HONO, and this was first order in NO₂ and H₂O
 (Alicke et al., 2002), and the conversion frequency of HONO ($k_{\text{HONO,het-night}}$) could be expressed as Equation 6. We
 determined the HONO formation by assuming a linear increase of its mixing ratio during a time interval (t_2-t_1). Since the
 mechanism summarized in R1 was first order in NO₂, the HONO formation was proportional to the NO₂ concentration. The
 255 conversion frequency was also assumed to be independent of gas phase water (Kleffmann et al., 1998), the average nighttime
 conversion frequency was determined by Equation 4,5, and 6. In order to eliminate the influence of direct emission and
 diffusion, CO was chosen as the reference species used for normalization:



$$k_{\text{HONO}}^0 = \frac{[\text{HONO}_{\text{corr,night}}]_{t_2} - [\text{HONO}_{\text{corr,night}}]_{t_1}}{(t_2 - t_1)[\text{NO}_2]} \quad (4)$$

$$260 \quad k_{HONO}^X = \frac{\left(\frac{[HONO_{corr,night}]_{t_2}}{[X]_{t_2}} - \frac{[HONO_{corr,night}]_{t_1}}{X_{t_1}}\right) \overline{[X]}}{0.5(t_2 - t_1) \left(\frac{[NO_2]_{t_2}}{[X]_{t_2}} + \frac{[NO_2]_{t_1}}{[X]_{t_1}}\right) \overline{[X]}} = \frac{2 \left(\frac{[HONO_{corr,night}]_{t_2}}{[X]_{t_2}} - \frac{[HONO_{corr,night}]_{t_1}}{X_{t_1}}\right)}{(t_2 - t_1) \left(\frac{[NO_2]_{t_2}}{[X]_{t_2}} + \frac{[NO_2]_{t_1}}{[X]_{t_1}}\right)} \quad (5)$$

$$k_{HONO,het-night} = \frac{1}{2} (k_{HONO}^0 + k_{HONO}^{CO}) \quad (6)$$

where $\overline{[NO_2]}$ was the mean value of NO_2 concentration between time t_2 and t_1 , k_{HONO}^0 was the conversion frequency which was not scaled, and k_{HONO}^X was the conversion frequency scaled with reference gases X (CO). Then the NO_2 to HONO conversion rate (k_{HONO}) was calculated by the combination of k_{HONO}^0 (not scaled k_{HONO}) and k_{HONO}^{CO} (CO scaled k_{HONO}), which could reduce the impact of uncertainties in diffusion process and emissions on the conversion rate.

Table 3. The conversion frequency k_{HONO} and $k_{HONO}[NO_2]$ in each month during the observation period.

	June	July	August	September	October
$k_{HONO,het-night}$ (hr^{-1})	0.011±0.003	0.01±0.002	0.0093±0.0015	0.0081±0.0006	0.0016±0.0002
$k_{HONO,het-night}[NO_2]$ (ppb/hr)	0.15±0.02	0.089±0.6%	0.079±0.004%	0.11±0.01	0.032±0.001

The averaged values of $k_{HONO,het-night}$ during the observation period were 0.011 hr^{-1} , 0.01 hr^{-1} , $0.0093\% \text{ hr}^{-1}$, 0.0081 hr^{-1} , and 0.0016 hr^{-1} , respectively, for June, July, August, September, and October, with 0.008 hr^{-1} on average. The averaged value was slightly higher than that reported by Xuan et al. (2023) and Jia et al. (2020), 0.0073 hr^{-1} and 0.0078 hr^{-1} from August to September, 2018. The varied values of k_{HONO} in each month indicated the different environmental conditions in each month, e.g., surface features, aerosol concentrations (Su et al., 2008). As shown in Table 3, June had the highest $k_{HONO,het-night}[NO_2]$ this indicated that the heterogeneous conversion from NO_2 was more important for HONO formation at night in June.

In general, the importance of the two generation pathways of nocturnal HONO might change due to the time and environmental factors. The North China has four distinct seasons, temperature and relative humidity varies with the seasons, pollutants in the gas phase and particle phase in the environment can also be affected, and the factors of observation location and observation time should be taken into account when evaluating the relative contribution of the generation pathways to HONO.

3.4 HONO daytime budget

3.4.1 Budget analysis of HONO

According to the source and sink pathways of HONO mentioned on introduction section, the sources of HONO on the daytime (10:00-15:00 LT) include: (1) direct emission of HONO (P_{emis}), (2) homogeneous reaction of NO with OH ($P_{OH+NO}=k_{OH+NO}[OH][NO]$), (3) the unknown sources during the daytime ($P_{unknown}$) (4) the vertical (T_v) and horizontal (T_h) transport processes of HONO. According to related observations (Wong et al., 2011; Wong et al., 2012; Wong et al., 2013; Pinto et al., 2014; Stutz et al., 2002; Wang et al., 2006; VandenBoer et al., 2013; Young et al., 2012), photolytic HONO formation at the ground is the major formation pathway in the lowest 20 m, while a combination of gas-phase, photolytic formation on aerosol, and vertical transport is responsible for daytime HONO between 200-300 meters above the ground. In

our work, the measurement was conducted on the rooftop of one building, about eight meters above the ground. As vertical exchange is unknown since the data to calculate its effect on HONO measured at 8 m is not available. Therefore, all subsequent analysis relies on the assumption that vertical exchange is unimportant, but this assumption represents an uncertainty that is not easily quantified; the sinks of HONO on the daytime include: (1) dry deposition of HONO ($L_{\text{dep}} = \frac{V_{\text{HONO}}}{H} [\text{HONO}]$), (2) photolysis of HONO ($L_{\text{phot}} = J_{\text{HONO}}[\text{HONO}]$), (3) reaction of OH with HONO ($L_{\text{OH+HONO}} = k_{\text{OH+HONO}}[\text{HONO}][\text{OH}]$).

The budget of HONO can be calculated by the following equation (8), (9), and (10):

$$\frac{d\text{HONO}}{dt} = (P_{\text{emis}} + P_{\text{OH+NO}} + P_{\text{unknown}}) - (L_{\text{dep}} + L_{\text{phot}} + L_{\text{OH+HONO}}) \quad (8)$$

$$P_{\text{unknown}} = \frac{d\text{HONO}}{dt} + L_{\text{dep}} + L_{\text{phot}} + L_{\text{OH+HONO}} - P_{\text{emis}} - P_{\text{OH+NO}} \quad (9)$$

$$P_{\text{unknown}} = \frac{\Delta\text{HONO}}{\Delta t} + k_{\text{OH+HONO}}[\text{OH}][\text{HONO}] + J_{\text{HONO}}[\text{HONO}] + \frac{V_{\text{HONO}}}{H} [\text{HONO}] - k_{\text{OH+NO}}[\text{OH}][\text{NO}] - P_{\text{emis}} \quad (10)$$

where $\frac{d\text{HONO}}{dt}$ represents the difference between HONO sources and sinks; $\frac{\Delta\text{HONO}}{\Delta t}$ was the observed change of HONO, the rate constants of $k_{\text{NO+OH}}$ and $k_{\text{HONO+OH}}$ at 298K were 9.8×10^{-12} and $6.0 \times 10^{-12} \text{ cm}^3 \text{ molecule}^{-1} \text{ s}^{-1}$, respectively (Liu et al., 2021a). A value of $V_{\text{HONO}} = 1.6 \text{ cm/s}$ was adopted here for the deposition rate of HONO (Zhang et al., 2019b), the value of $H = 200 \text{ m}$ was used here as the mixing layer height (Hu et al., 2022). The OH concentration and J_{HONO} were calculated with the method mentioned in section 2.2. According to the model simulation results, the averaged J_{HONO} values were in the range of $0.78 \times 10^{-3} - 1.4 \times 10^{-3} \text{ s}^{-1}$. The daytime hourly averaged values of OH concentration in the five months were in the ranges of $2.9 \times 10^6 - 8.9 \times 10^6 \text{ molecules/cm}^3$.

Figure 4 illustrated the details production/loss rates and proportion of HONO during the observation period. And Table S3 showed the averaged production/loss rates of HONO around noontime (10:00-15:00 LT). The dominant loss pathway of HONO during the five months was the photodecomposition (L_{phot}), the averaged values of L_{phot} were 1.1-3.9 ppb/hr around noontime. The following loss pathway of HONO was dry deposition (L_{dep}), the averaged values of L_{dep} were 0.13-0.27 ppb/hr around noontime. The loss pathway with the least contribution was the reaction of OH with HONO ($L_{\text{OH+HONO}}$), the averaged values of $L_{\text{OH+HONO}}$ were 0.029-0.15 ppb/hr at the same time. For the production pathways of HONO around noontime, the averaged values of homogeneous reaction rate between NO and OH ($P_{\text{OH+NO}}$) were 0.64-1.5 ppb/hr. The averaged values of P_{emis} were 0.16-0.33 ppb/hr. For the high value of P_{emis} in October, the possible reasons maybe that the corresponding diffusion conditions were weakened due to the decrease in wind speed, and the change of epidemic control policies in this area in October resulted in the increase of the traffic emissions. The averaged values of P_{unknown} were 0.29-2.7 ppb/hr, the contribution of which to the production of HONO were 78% (June), 55% (July), 64% (August), 68% (September), and 30% (October), respectively. In summary, photodecomposition was the largest removal pathway around noontime during the whole observation period; P_{unknown} contributed the most to the production of HONO in June, July, August, and

September, homogeneous reaction of NO and OH dominated the HONO production in October at daytime; June had the highest P_{unknown} , and October had the lowest P_{unknown} .

The obtained average P_{unknown} values in Summer (from June to August), 2.3 ppb/hr, was at the middle level of those reported literatures in urban areas, as shown in Table 4. The P_{unknown} values in Autumn (from September to October) (1.0 ppb/hr) was at the lower-middle level of those reported literatures in urban areas.

Table 4. The P_{unknown} values in this work and reported literatures.

	Date	value (ppb/h)	location	literatures
Summer	18 August to 16 September, 2018	0.49	Beijing	Xuan et al., 2023
	June to July, 2019	0.59	Beijing	Li et al., 2021
	24 July to 6 August, 2015	0.75	Xi'an	Huang et al., 2017
	1 June to 31 August, 2018	0.98	Nanjing	Liu et al., 2019
	8-20 March, 2005	1.7	Santiago	Elshorbany et al., 2009
	June to August, 2021	2.3	Beijing	This work
	25 May to 15 July, 2018	2.1	Beijing	Liu et al., 2021a
	1 June to 31 August, 2016	3.0	Jinan	Li et al., 2018
	20 June to 25 July, 2016	3.8	Beijing	Wang et al., 2017a
	August, 2018	4.5	Xiamen	Hu et al., 2022
Autumn	27 September to 9 November, 2018	0.65	Guangzhou	Yu et al., 2022b
	September to October, 2021	1.1	Beijing	This work
	October, 2018	2.1	Xiamen	Hu et al., 2022
	23 August to 17 September, 2018	2.3	Beijing	Jia et al., 2020
	22 September to 21 October, 2015	3.1	Beijing	Wang et al., 2017a

325

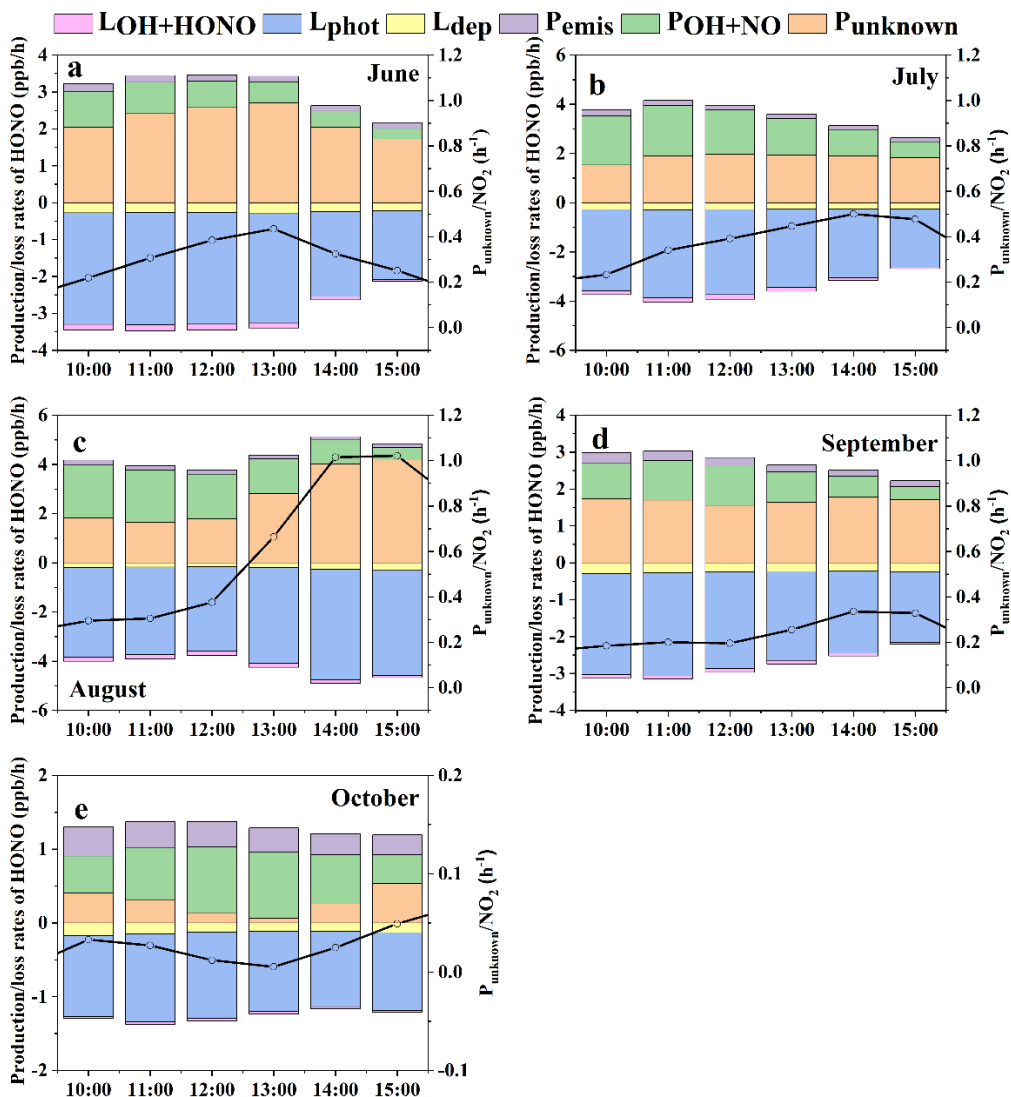


Figure 4. Daytime HONO budget in average production (P_{emis} , $P_{\text{NO+OH}}$, P_{unknown}) and loss rates ($L_{\text{OH+HONO}}$, L_{phot} , L_{dep}) during the five months.

3.4.2 Possible unknown source at daytime

330 Based on the assumption that nighttime heterogeneous conversion of NO_2 continued in the same way at the daytime, the nighttime heterogeneous production of HONO was adopted here, and $P_{\text{het}} = k_{\text{HONO}}[\text{NO}_2]$ (Alicke, 2002; Sörgel et al., 2011). Dark heterogeneous formation accounted for 6.5% (June), 4.9% (July), 2.9% (August), 6.5% (September), and 11% (October) of missing sources of HONO at daytime, respectively, which was almost negligible at daytime. And the average value of P_{unknown} normalized by NO_2 at daytime (10:00-15:00 LT) was 0.025-0.61 h^{-1} , as shown in Table S3, much greater

335 than the conversion rates at nighttime. This phenomenon implied that P_{unknown} could not be explained by the nocturnal mechanism of NO_2 to HONO.

According to the reported possible HONO sources in literatures (Zhang et al., 2023c; Zhang et al., 2022; Lian et al., 2022), light-induced heterogeneous conversion from NO_2 to HONO and photolysis of nitrate were responsible for the P_{unknown} , solar illumination and relative humidity were the two most frequently considered meteorological factors. Thus, a
340 correlation analysis was performed to explore the potential unknown sources of HONO at daytime, and the details are shown in Table S4.

Wang et al. (2017a) analysed the data of Beijing from 20 June to 25 July 2016 (summer) and found that, compared to JNO_2 or RH alone, the correlation between P_{unknown} and product of JNO_2 and RH was good. Based on this phenomenon, it was thought that photolytic and heterogeneous reaction occurring upon wet surface were important unknown sources of
345 HONO. In our work, good correlation between P_{unknown} and product of JNO_2 and RH was found in June. However, this phenomenon was not evident in other four months. The phenomenon was not evident in four of the five months, this showed that in this observation there was not strong evidence for this conclusion. As shown in Table S4, June had the lowest RH and the highest JNO_2 value, the other four months had relative higher RH (due to the precipitation) and lower JNO_2 value. This phenomenon may be closely related to meteorological conditions and requires further research for validation.

350 In August and September, it could be seen that low NO_2 and $\text{PM}_{2.5}$ conditions could lead to high P_{unknown} , corresponding to high JNO_2 value and relatively low RH (20-40%). This phenomenon suggested that there were other possible unknown sources of HONO, and this might be due to the light-enhancing effect of NO_2 on non-aerosol surfaces.

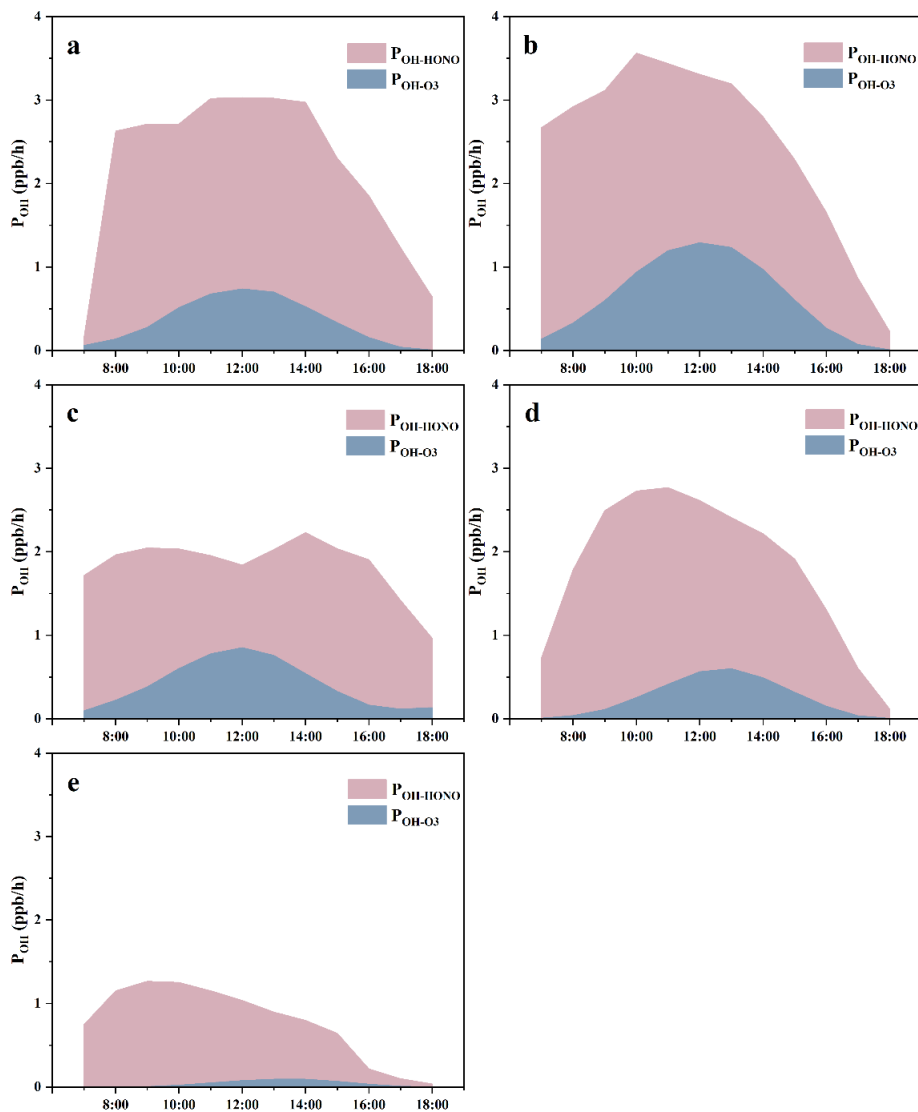
Through heterogeneous photochemical simulation experiments, Wingen et al. (2008) found that an enhanced NO_2 yield was observed as the chloride to nitrate ratio increased. Jin et al. (2022) performed the nitrate photolysis experiments with a
355 flow tube reactor, and found that surprising yields of HONO and NO were formed during the photolysis experiment of NH_4NO_3 in the presence of halogen ions (Cl^- , Br^- , I^-), this phenomenon indicated the important role of halogen ions in nitrate photolysis process. Thus, we analysed the correlation between nitrate and P_{unknown} in the presence of Cl^- ion. As shown in Table S4, the correlation between P_{unknown} and the corresponding factors was as follows: $\text{JNO}_2 \times [\text{NO}_3^-] \times \text{Cl}^-$ ($R = 0.46$, $P < 0.05$) $>$ $\text{JNO}_2 \times [\text{NO}_3^-]$ ($R = 0.29$, $P < 0.05$) in July; $\text{JNO}_2 \times [\text{NO}_3^-] \times \text{RH} \times \text{Cl}^-$ ($R = 0.44$, $P < 0.05$) $>$ $\text{JNO}_2 \times [\text{NO}_3^-] \times \text{RH}$
360 ($R = 0.30$, $P < 0.05$) in July. Bao et al. (2018) found that a large amount of HONO and NO_x were formed during the photolysis experiment of nitrate in the presence of sulfate. Significant positive correlations also occurred in our observations in July: $\text{JNO}_2 \times [\text{NO}_3^-] \times \text{SO}_4^{2-}$ ($R = 0.32$, $P < 0.05$) $>$ $\text{JNO}_2 \times [\text{NO}_3^-]$ ($R = 0.29$, $P < 0.05$); $\text{JNO}_2 \times [\text{NO}_3^-] \times \text{RH} \times \text{SO}_4^{2-}$ ($R = 0.33$, $P < 0.05$) $>$ $\text{JNO}_2 \times [\text{NO}_3^-] \times \text{RH}$ ($R = 0.30$, $P < 0.05$). Yang et al. (2018) and Ye et al. (2019) found that the presence of organic components significantly enhanced the denitrification rate of nitrate. In this work, organic carbon (OC) was used as a
365 proxy for organic components, and the correlation was analysed. As shown in Table S4, the enhancement of the correlation between P_{unknown} and NO_3^- in the presence of OC was observed, $\text{JNO}_2 \times [\text{NO}_3^-] \times \text{OC}$ ($R = 0.55$, $P < 0.05$) $>$ $\text{JNO}_2 \times [\text{NO}_3^-]$

($R = 0.48$, $P < 0.05$) in June. However, the phenomenon above were not evident in four of the five months, this showed that in this observation there was not strong evidence for these conclusions, but that they could contribute based on prior literatures.

3.4.3 OH production rate at daytime

370 As HONO was the efficient source of OH radical at daytime (Zhang et al., 2023c; Yu et al., 2022b), the OH production rate from HONO ($P_{\text{OH-HONO}}$) at the CRAES observation site was calculated in this work. As the formaldehyde was not measured in this work, which was a large and known HO_x source in urban areas, thus the analysis here was not a full HO_x budget.

Figure 5 showed that the OH production rate from HONO usually occurred before noontime, and this was caused by the existing HONO and its photolysis, this phenomenon was obvious in July, September, and October. And for $P_{\text{OH-O}_3}$ (the
375 production rate of OH radical via O_3 photolysis to O^1D followed by reaction with water vapor), the highest value was around noontime, which coincided with $J(\text{O}^1\text{D})$ trend, this phenomenon was obvious in June, July, and August. In September and October (autumn), the highest value of $P_{\text{OH-O}_3}$ occurred a little later after noontime. The average $P_{\text{OH-HONO}}$ during 8:00-16:00 LT was 2.7 ppb/h (June), 2.9 ppb/h (July), 2.0 ppb/h (August), 2.3 ppb/h (September), and 0.93 ppb/h (October), respectively; And the average $P_{\text{OH-O}_3}$ during 8:00-16:00 LT was 0.45 ppb/h (June), 0.82 ppb/h (July), 0.51 ppb/h (August), 0.33 ppb/h
380 (September), and 0.048 ppb/h (October), respectively; the contribution of HONO to OH was significantly greater than that of ozone. The important role of HONO to OH in the atmospheric oxidizing capacity should benefit the production of photochemical ozone (Xuan et al., 2023; Jia et al., 2023; Zhang et al., 2023b; Zhang et al., 2022), the formation of new particles (Stolzenburg et al., 2023), and the formation of secondary aerosols (Zhang et al., 2023c; Xuan et al., 2023; Liu et al., 2021a).



385

Figure 5. Averaged OH production rates from photolysis of HONO and ozone in (a) June, (b) July, (c) August, (d) September, and (e) October.

3.5 The correlations between HONO, $PM_{2.5}$, and O_3

In view of the importance of HONO to atmospheric oxidizing capacity (Zhong et al., 2023; Zhang et al., 2023b; Song et al., 2023), the correlations between HONO, $PM_{2.5}$, and O_3 were analysed. According to the Technical Regulation on Ambient Air Quality Index (on trial) in China (633—2012, 2012), $PM_{2.5}$ concentrations were divided into three zones: $\leq 35 \mu\text{g}/\text{m}^3$, 35-75 $\mu\text{g}/\text{m}^3$, and $\geq 75 \mu\text{g}/\text{m}^3$; and analysed at nighttime and daytime, respectively.

As shown in Figure 6, $PM_{2.5}$ concentrations were positively correlated with HONO, i.e., the increase of $PM_{2.5}$ pollution was accompanied by the increase of HONO concentration during the daytime. At night, except in September, the same

395 pattern was presented. One possible explanation of this phenomenon was that the increase in particle pollution in summer and autumn might lead to the formation of HONO and an increase in its concentration. Another possible explanation was that high HONO concentrations could lead to higher oxidative capacity and therefore higher rates of aerosol formation. There was also a possible explanation as both PM_{2.5} and HONO were stem from the same sources (i.e., their concentrations would both increase during pollution events). However, when it came to ozone, we could see a different phenomenon. In 400 June and July, ozone showed a decreasing trend as particle and HONO concentrations increased during the daytime, but when at night, ozone concentrations tend to increase. In August and September, ozone showed an increasing trend as particle and HONO concentration increased both during the daytime and nighttime. In October, ozone showed an increasing trend at daytime, but a decreasing trend at night. Wang et al. (2017b) summarized the ozone abundance and its relationship to chemical processes and atmospheric dynamics in China, the ozone formation and concentration could be affected by various 405 factors, including precursors, meteorological factors, and regional transport, et al., the formation of OH radical by HONO photolysis was a pathway involved in the RO_x and NO_x cycle of ozone formation, ozone was not directly related to HONO.

Wang et al. (2023a) analysed the relationships between ozone, PM_{2.5}, and mixing layer height in warm season, and found that the enhanced atmospheric oxidant capacity could promote the secondary transformation of particles, and weakened the dilution effect of mixing layer height rise on pollutants. The contribution of observed HONO to atmospheric 410 oxidant capacity exceeded that of ozone, so it was necessary to pay more attention to the sources of HONO in warm season.

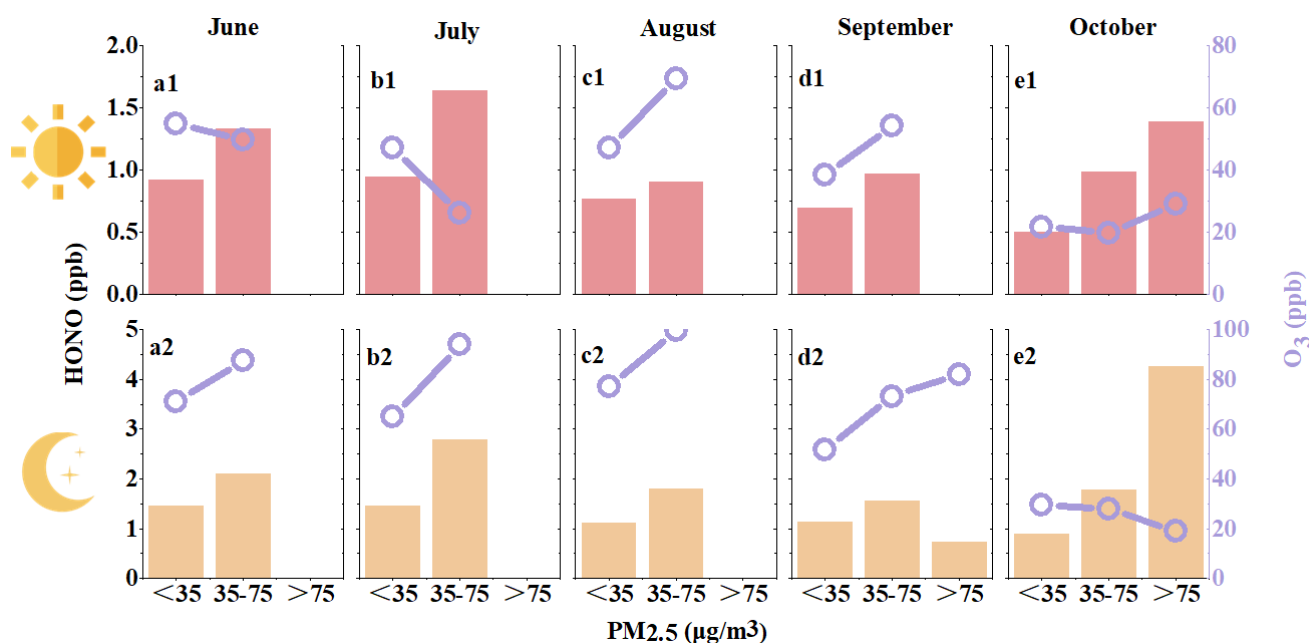


Figure 6. Distributions of HONO and O₃ mean concentrations under different PM_{2.5} pollution conditions. The upper panel was the daytime average value (7:00-18:00 LT), and the bottom panel was the nighttime average value (19:00-6:00 LT).

4 Conclusions

415 Continuous field observation of HONO in warm seasons was conducted in an urban site of Beijing, from June to October
2021. The monthly average HONO concentration was in the range of 0.89-1.28 ppb, showing a larger contribution to OH
radical relative to ozone at daytime, above three times as that of ozone in each month. Compared with previous field
observations in the urban sites of Beijing, the contribution of vehicle emissions to HONO (0.017) was relatively high. The
monthly nocturnal conversion rate of NO₂ to HONO was in the range of 0.0016-0.011 hr⁻¹, accounted for 2.9%-11% of
420 missing sources of HONO at daytime; the average value of P_{unknown} normalized by NO₂ at daytime (10:00-15:00 LT) was
0.025-0.61 hr⁻¹, much greater than the conversion rates at nighttime, which indicated that nocturnal heterogeneous
conversion from NO₂ to HONO was almost negligible at daytime.

Based on the field observations in summer and winter, Liu et al. (2021b) evaluated the atmospheric oxidizing capacity
in the megacity of Beijing, and found that the atmospheric oxidizing capacity showed a clear seasonal pattern, which was
425 stronger in summer than that in winter. The dominant oxidant contributor to atmospheric oxidizing capacity at daytime was
OH radical, and ozone was the second most important oxidant. Our work showed that in summer and autumn, the
contribution of HONO to OH radical was significantly greater than that of ozone, this further illustrated the importance of
HONO. As mentioned in Section 3.4.1, the contributions of P_{unknown} to the production of HONO were 78% (June), 55%
(July), 64% (August), 68% (September), and 30% (October), respectively. According to the OH production from HONO, the
430 OH production rate from the missing HONO was also very important to atmospheric oxidation capacity. Thus, further
investigation was required to figure out the source of HONO. In recent years, the concentration of atmospheric particulate
matter in China decreased significantly, but the ozone concentration showed a fluctuating upward trend, the atmospheric
oxidation capacity increased significantly, especially in the warm season. Given the contribution of HONO to atmospheric
oxidation capacity, its sources should be studied in more detail.

435

Code and data availability. The data used in this study are available upon request from the corresponding author.

Author contributions. JLL and HL conceived and led the studies. JLL, CFL, HZ, WGW, and HL performed observation
studies and data analysis. MML, YXY, YFS, CC, YCG, YSX, JG, and MFG discussed the results and commented on the
paper. JLL prepared the article with contributions from all co-authors.

440 **Competing interests.** The authors declare that they have no conflict of interest.

Financial support. This research has been supported by National Key Research and Development Program of China (No.
2023YFC3706102), National Natural Science Foundation of China (NSFC, No. 41931287, No.42130606, No. 42405104, No.
42175133, No. 42307139).

445 References

- Alicke, B.: Impact of nitrous acid photolysis on the total hydroxyl radical budget during the Limitation of Oxidant Production/Pianura Padana Produzione di Ozono study in Milan, *J. Geophys. Res.*, 107, 8196, doi: 10.1029/2000jd000075, 2002.
- 450 Andrae, M. O.: Emission of trace gases and aerosols from biomass burning – an updated assessment, *Atmos. Chem. Phys.*, 19, 8523–8546, doi: 10.5194/acp-19-8523-2019, 2019.
- Aubin, D. G., and Abbatt, J. P. D.: Interaction of NO₂ with hydrocarbon soot: Focus on HONO yield, surface modification, and mechanism, *J. Phys. Chem. A*, 111, 6263–6273, doi: 10.1021/jp068884h, 2007.
- Bao, F. X., Li, M., Zhang, Y., Chen, C. C., and Zhao, J. C.: Photochemical aging of Beijing urban PM_{2.5}: HONO production, *Environ. Sci. Technol.*, 52, 6309–6316, doi: 10.1021/acs.est.8b00538, 2018.
- 455 Bhattarai, H. R., Wanek, W., Siljanen, H. M. P., Ronkainen, J. G., Liimatainen, M., Hu, Y., Nykänen, H., Biasi, C., and Maljanen, M.: Denitrification is the major nitrous acid production pathway in boreal agricultural soils, *Commun. Earth Environ.*, 2, doi: 10.1038/s43247-021-00125-7, 2021.
- Cao, Y., Ma, Q., Chu, B., and He, H.: Homogeneous and heterogeneous photolysis of nitrate in the atmosphere: state of the science, current research needs, and future prospects, *Front. Environ. Sci. Eng.*, 17, doi: 10.1007/s11783-023-1648-6, 2022.
- 460 Chen, D. Y., Zhou, L., Liu, S., Lian, C. F., Wang, W. G., Liu, H. F., Li, C. Y., Liu, Y. L., Luo, L., Xiao, K., Chen, Y., Qiu, Y., Tan, Q. W., Ge, M. F., and Yang, F. M.: Primary sources of HONO vary during the daytime: Insights based on a field campaign, *Sci. Total. Environ.*, 903, 12, doi: 10.1016/j.scitotenv.2023.166605, 2023.
- Chen, Y., Wang, W., Lian, C., Peng, C., Zhang, W., Li, J., Liu, M., Shi, B., Wang, X., and Ge, M.: Evaluation and impact factors of indoor and outdoor gas-phase nitrous acid under different environmental conditions, *J. Environ. Sci. (China)*, 95, 165–171, doi: 10.1016/j.jes.2020.03.048, 2020.
- 465 Cox, R. A., Dervent, G. K., and Holt, P. M.: Relative rate constants for the reactions of OH radicals with H₂, CH₄, CO, NO, and HONO at atmospheric pressure and 296 K, *J. Chem. Soc., Faraday Trans. 1*, 72, 2031–2043, doi: 10.1039/f19767202031, 1976.
- 470 Czader, B. H., Rappenglück, B., Percell, P., Byun, D. W., Ngan, F., and Kim, S.: Modeling nitrous acid and its impact on ozone and hydroxyl radical during the Texas Air Quality Study 2006, *Atmos. Chem. Phys.*, 12, 6939–6951, doi: 10.5194/acp-12-6939-2012, 2012.
- Du, C. L., Liu, S. Y., Yu, X., Li, X. M., Chen, C., Peng, Y., Dong, Y., Dong, Z. P., and Wang, F. Q.: Urban boundary layer height characteristics and relationship with particulate matter mass concentrations in Xi'an, Central China, *Aerosol Air Qual. Res.*, 13, 1598–1607, doi: 10.4209/aaqr.2012.10.0274, 2013.
- 475 El Zein, A., Romanias, M. N., and Bedjanian, Y.: Kinetics and products of heterogeneous reaction of HONO with Fe₂O₃ and Arizona Test Dust, *Environ. Sci. Technol.*, 47, 6325–6331, doi: 10.1021/es400794c, 2013.
- Elshorbany, Y. F., Kurtenbach, R., Wiesen, P., Lissi, E., Rubio, M., Villena, G., Gramsch, E., Rickard, A. R., Pilling, M. J., and Kleffmann, J.: Oxidation capacity of the city air of Santiago, Chile, *Atmos. Chem. Phys.*, 9, 2257–2273, doi: 10.5194/acp-9-2257-2009, 2009.
- 480 Elshorbany, Y. F., Steil, B., Brühl, C., and Lelieveld, J.: Impact of HONO on global atmospheric chemistry calculated with an empirical parameterization in the EMAC model, *Atmos. Chem. Phys.*, 12, 9977–10000, doi: 10.5194/acp-12-9977-2012, 2012.
- Finlayson-Pitts, B. J., Wingen, L. M., Sumner, A. L., Syomin, D., and Ramazan, K. A.: The heterogeneous hydrolysis of NO₂ in laboratory systems and in outdoor and indoor atmospheres: An integrated mechanism, *Phys. Chem. Chem. Phys.*, 5, 223–242, doi: 10.1039/b208564j, 2003.
- 485 Gen, M., Liang, Z., Zhang, R., Go Mabato, B. R., and Chan, C. K.: Particulate nitrate photolysis in the atmosphere, *Environ. Sci.: Atmos.*, 2, 111–127, doi: 10.1039/d1ea00087j, 2022.
- Gen, M. S., Zhang, R. F., Huang, D. D., Li, Y. J., and Chan, C. K.: Heterogeneous SO₂ oxidation in sulfate formation by photolysis of particulate nitrate, *Environ. Sci. Technol. Lett.*, 6, 86–91, doi: 10.1021/acs.estlett.8b00681, 2019.
- 490 Gu, R., Shen, H., Xue, L., Wang, T., Gao, J., Li, H., Liang, Y., Xia, M., Yu, C., Liu, Y., and Wang, W.: Investigating the sources of atmospheric nitrous acid (HONO) in the megacity of Beijing, China, *Sci. Total. Environ.*, 812, 152270, doi: 10.1016/j.scitotenv.2021.152270, 2022.

- 495 Hendrick, F., Müller, J. F., Clémer, K., Wang, P., De Mazière, M., Fayt, C., Gielen, C., Hermans, C., Ma, J. Z., Pinardi, G., Stavrou, T., Vlemmix, T., and Van Roozendaal, M.: Four years of ground-based MAX-DOAS observations of HONO and NO₂ in the Beijing area, *Atmos. Chem. Phys.*, 14, 765–781, doi: 10.5194/acp-14-765-2014, 2014.
- Hou, S., Tong, S., Ge, M., and An, J.: Comparison of atmospheric nitrous acid during severe haze and clean periods in Beijing, China, *Atmos. Environ.*, 124, 199–206, doi: 10.1016/j.atmosenv.2015.06.023, 2016.
- 500 Hu, B., Duan, J., Hong, Y., Xu, L., Li, M., Bian, Y., Qin, M., Fang, W., Xie, P., and Chen, J.: Exploration of the atmospheric chemistry of nitrous acid in a coastal city of southeastern China: results from measurements across four seasons, *Atmos. Chem. Phys.*, 22, 371–393, doi: 10.5194/acp-22-371-2022, 2022.
- Hu, M., Zhou, F., Shao, K., Zhang, Y., Tang, X., and Slanina, J.: Diurnal variations of aerosol chemical compositions and related gaseous pollutants in Beijing and Guangzhou, *J. Environ. Sci. Health A*, 37, 479–488, doi: 10.1081/ese-120003229, 2002.
- 505 Huang, J., Pan, X., Guo, X., and Li, G.: Health impact of China's Air Pollution Prevention and Control Action Plan: An analysis of national air quality monitoring and mortality data, *Lancet Planet. Health*, 2, e313–e323, doi: 10.1016/S2542-5196(18)30141-4, 2018.
- Huang, R.-J., Yang, L., Cao, J., Wang, Q., Tie, X., Ho, K.-F., Shen, Z., Zhang, R., Li, G., Zhu, C., Zhang, N., Dai, W., Zhou, J., Liu, S., Chen, Y., Chen, J., and O'Dowd, C. D.: Concentration and sources of atmospheric nitrous acid (HONO) at an urban site in Western China, *Sci. Total Environ.*, 593, 165–172, doi: 10.1016/j.scitotenv.2017.02.166, 2017.
- 510 Jia, C., Tong, S., Zhang, X., Li, F., Zhang, W., Li, W., Wang, Z., Zhang, G., Tang, G., Liu, Z., and Ge, M.: Atmospheric oxidizing capacity in autumn Beijing: Analysis of the O₃ and PM_{2.5} episodes based on observation-based model, *J. Environ. Sci. (China)*, 124, 557–569, doi: 10.1016/j.jes.2021.11.020, 2023.
- Jia, C. H., Tong, S. R., Zhang, W. Q., Zhang, X. R., Li, W. R., Wang, Z., Wang, L. L., Liu, Z. R., Hu, B., Zhao, P. S., and Ge, M. F.: Pollution characteristics and potential sources of nitrous acid (HONO) in early autumn 2018 of Beijing, *Sci. Total Environ.*, 735, 11, doi: 10.1016/j.scitotenv.2020.139317, 2020.
- 515 Jin, S., Kong, L., Yang, K., Wang, C., Xia, L., Wang, Y., Tan, J., and Wang, L.: Combined effects of high relative humidity and ultraviolet irradiation: Enhancing the production of gaseous NO₂ from the photolysis of NH₄NO₃, *Sci. Total Environ.*, 838, 156480, doi: 10.1016/j.scitotenv.2022.156480, 2022.
- 520 Keller-Rudek, H., Moortgat, G. K., Sander, R., and Sørensen, R.: The MPI-Mainz UV/VIS spectral atlas of gaseous molecules of atmospheric interest, *Earth Syst. Sci. Data*, 5, 365–373, doi: 10.5194/essd-5-365-2013, 2013.
- Kessler, C., and Platt, U.: Nitrous acid in polluted air masses—Sources and formation pathways, *Physico-Chemical Behaviour of Atmospheric Pollutants*, Springer, Dordrecht., 412–422, doi: 10.1007/978-94-009-6505-8_44, 1984.
- Kirchstetter, T. W., Harley, R. A., and Littlejohn, D.: Measurement of nitrous acid in motor vehicle exhaust, *Environ. Sci. Technol.*, 30, 2843–2849, doi: 10.1021/es960135y, 1996.
- 525 Kleffmann, J., Becker, K. H., and Wiesen, P.: Heterogeneous NO₂ conversion processes on acid surfaces: Possible atmospheric implications, *Atmos. Environ.*, 32, 2721–2729, doi: 10.1016/s1352-2310(98)00065-x, 1998.
- Kurtenbach, R., Becker, K. H., Gomes, J. A. G., Kleffmann, J., Lörzer, J. C., Spittler, M., Wiesen, P., Ackermann, R., and Geyher, U. P.: Investigations of emissions and heterogeneous formation of HONO in a road traffic tunnel, *Atmos. Environ.*, 35, 3385–3394, doi: 10.1016/S1352-2310(01)00138-8, 2001.
- 530 Li, C., Hammer, M. S., Zheng, B., and Cohen, R. C.: Accelerated reduction of air pollutants in China, 2017–2020, *Sci. Total Environ.*, 803, 150011, doi: 10.1016/j.scitotenv.2021.150011, 2022.
- Li, D., Xue, L., Wen, L., Wang, X., Chen, T., Mellouki, A., Chen, J., and Wang, W.: Characteristics and sources of nitrous acid in an urban atmosphere of northern China: Results from 1-yr continuous observations, *Atmos. Environ.*, 182, 296–306, doi: 10.1016/j.atmosenv.2018.03.033, 2018.
- 535 Li, X., Brauers, T., Häsel, R., Bohn, B., Fuchs, H., Hofzumahaus, A., Holland, F., Lou, S., Lu, K. D., Rohrer, F., Hu, M., Zeng, L. M., Zhang, Y. H., Garland, R. M., Su, H., Nowak, A., Wiedensohler, A., Takegawa, N., Shao, M., and Wahner, A.: Exploring the atmospheric chemistry of nitrous acid (HONO) at a rural site in Southern China, *Atmos. Chem. Phys.*, 12, 1497–1513, doi: 10.5194/acp-12-1497-2012, 2012.
- 540 Li, Y., Wang, X., Wu, Z., Li, L., Wang, C., Li, H., Zhang, X., Zhang, Y., Li, J., Gao, R., Xue, L., Mellouki, A., Ren, Y., and Zhang, Q.: Atmospheric nitrous acid (HONO) in an alternate process of haze pollution and ozone pollution in urban Beijing in summertime: Variations, sources and contribution to atmospheric photochemistry, *Atmos. Res.*, 260, 105689, doi: 10.1016/j.atmosres.2021.105689, 2021.

- 545 Lian, C., Wang, W., Chen, Y., Zhang, Y., Zhang, J., Liu, Y., Fan, X., Li, C., Zhan, J., Lin, Z., Hua, C., Zhang, W., Liu, M., Li, J., Wang, X., An, J., and Ge, M.: Long-term winter observation of nitrous acid in the urban area of Beijing, *J. Environ. Sci. (China)*, 114, 334–342, doi: 10.1016/j.jes.2021.09.010, 2022.
- Liao, S., Zhang, J., Yu, F., Zhu, M., Liu, J., Ou, J., Dong, H., Sha, Q., Zhong, Z., Xie, Y., Luo, H., Zhang, L., and Zheng, J.: High gaseous nitrous acid (HONO) emissions from light-duty diesel vehicles, *Environ. Sci. Technol.*, 55, 200–208, doi: 10.1021/acs.est.0c05599, 2021.
- 550 Lin, D., Tong, S., Zhang, W., Li, W., Li, F., Jia, C., Zhang, G., Chen, M., Zhang, X., Wang, Z., Ge, M., and He, X.: Formation mechanisms of nitrous acid (HONO) during the haze and non-haze periods in Beijing, China, *J. Environ. Sci. (China)*, 114, 343–353, doi: 10.1016/j.jes.2021.09.013, 2022.
- Liu, J., Liu, Z., Ma, Z., Yang, S., Yao, D., Zhao, S., Hu, B., Tang, G., Sun, J., Cheng, M., Xu, Z., and Wang, Y.: Detailed budget analysis of HONO in Beijing, China: Implication on atmosphere oxidation capacity in polluted megacity, *Atmos. Environ.*, 244, 117957, doi: 10.1016/j.atmosenv.2020.117957, 2021a.
- 555 Liu, J. P., Deng, H. F., Li, S., Jiang, H. Y., Mekic, M., Zhou, W. T., Wang, Y. Q., Loisel, G., Wang, X. M., and Gligorovski, S.: Light-enhanced heterogeneous conversion of NO₂ to HONO on solid films consisting of Fluorene and Fluorene/Na₂SO₄: An impact on urban and indoor atmosphere, *Environ. Sci. Technol.*, 54, 11079–11086, doi: 10.1021/acs.est.0c02627, 2020.
- 560 Liu, J. P., Li, B., Deng, H. F., Yang, Y., Song, W., Wang, X. M., Luo, Y. M., Francisco, J. S., Li, L., and Gligorovski, S.: Resolving the formation mechanism of HONO via Ammonia-Promoted photosensitized conversion of monomeric NO₂ on urban glass surfaces, *J. Am. Chem. Soc.*, 145, 11488–11493, doi: 10.1021/jacs.3c02067, 2023a.
- Liu, Y., Nie, W., Xu, Z., Wang, T., Wang, R., Li, Y., Wang, L., Chi, X., and Ding, A.: Semi-quantitative understanding of source contribution to nitrous acid (HONO) based on 1 year of continuous observation at the SORPES station in eastern China, *Atmos. Chem. Phys.*, 19, 13289–13308, doi: 10.5194/acp-19-13289-2019, 2019.
- 565 Liu, Y., Geng, G., Cheng, J., Liu, Y., Xiao, Q., Liu, L., Shi, Q., Tong, D., He, K., and Zhang, Q.: Drivers of increasing ozone during the two phases of Clean Air Actions in China 2013–2020, *Environ. Sci. Technol.*, 57, 8954–8964, doi: 10.1021/acs.est.3c00054, 2023b.
- Liu, Z., Wang, Y., Hu, B., Lu, K., Tang, G., Ji, D., Yang, X., Gao, W., Xie, Y., Liu, J., Yao, D., Yang, Y., and Zhang, Y.: Elucidating the quantitative characterization of atmospheric oxidation capacity in Beijing, China, *Sci. Total Environ.*, 771, 145306, doi: 10.1016/j.scitotenv.2021.145306, 2021b.
- Murthy, B. S., Latha, R., Tiwari, A., Rathod, A., Singh, S., and Beig, G.: Impact of mixing layer height on air quality in winter, *J Atmos. Sol Terr Phys*, 197, 105157, doi: 10.1016/j.jastp.2019.105157, 2020.
- 575 Nie, W., Ding, A. J., Xie, Y. N., Xu, Z., Mao, H., Kerminen, V. M., Zheng, L. F., Qi, X. M., Huang, X., Yang, X. Q., Sun, J. N., Herrmann, E., Petäjä, T., Kulmala, M., and Fu, C. B.: Influence of biomass burning plumes on HONO chemistry in eastern China, *Atmos. Chem. Phys.*, 15, 1147–1159, doi: 10.5194/acp-15-1147-2015, 2015.
- Pinto, J.P., J. Dibb, B.H. Lee, B. Rappenglück, E.C. Wood, M. Levy, R.Y. Zhang, B. Lefer, X.R. Ren, J. Stutz, C. Tsai, L. Ackermann, J. Golovko, S.C. Herndon, M. Oakes, Q.Y. Meng, J.W. Munger, M. Zahniser, and J. Zheng, Intercomparison of Field Measurements of Nitrous Acid (HONO) during the SHARP Campaign. *Journal of Geophysical Research: Atmospheres*, 2014: p. 2013JD020287.
- 580 Ren, Y., Wei, J., Wang, G., Wu, Z., Ji, Y., and Li, H.: Evolution of aerosol chemistry in Beijing under strong influence of anthropogenic pollutants: Composition, sources, and secondary formation of fine particulate nitrated aromatic compounds, *Environ. Res.*, 204, 111982, doi: 10.1016/j.envres.2021.111982, 2022.
- 585 Requia, W. J., Higgins, C. D., Adams, M. D., Mohamed, M., and Koutrakis, P.: The health impacts of weekday traffic: A health risk assessment of PM_{2.5} emissions during congested periods, *Environ. Int.*, 111, 164–176, doi: 10.1016/j.envint.2017.11.025, 2018.
- Romanias, M. N., El Zein, A., and Bedjanian, Y.: Reactive uptake of HONO on aluminium oxide surface, *J. Photochem. Photobiol. A*, 250, 50–57, doi: 10.1016/j.jphotochem.2012.09.018, 2012.
- 590 Rohrer, F., and Berresheim, H.: Strong correlation between levels of tropospheric hydroxyl radicals and solar ultraviolet radiation, *Nature*, 442, 184–187, 10.1038/nature04924, 2006.
- Rohrer, F., Lu, K., Hofzumahaus, A., Bohn, B., Brauers, T., Chang, C.-C., Fuchs, H., Häseler, R., Holland, F., Hu, M., Kita, K., Kondo, Y., Li, X., Lou, S., Oebel, A., Shao, M., Zeng, L., Zhu, T., Zhang, Y., and Wahner, A.: Maximum efficiency in the hydroxyl radical-based self-cleansing of the troposphere, *Nat. Geosci.*, 7, 559–563,

- <https://doi.org/10.1038/ngeo2199>, 2014.
- 595 Sörgel, M., Regelin, E., Bozem, H., Diesch, J. M., Drewnick, F., Fischer, H., Harder, H., Held, A., Hosaynali-Beygi, Z., Martinez, M., and Zetzsch, C.: Quantification of the unknown HONO daytime source and its relation to NO₂, *Atmos. Chem. Phys.*, 11, 10433–10447, doi: 10.5194/acp-11-10433-2011, 2011.
- Simoneit, B. R. T.: Biomass burning - A review of organic tracers for smoke from incomplete combustion, *Appl. Geochem.*, 17, 129–162, doi: 10.1016/S0883-2927(01)00061-0, 2002.
- 600 Song, M., Zhao, X., Liu, P., Mu, J., He, G., Zhang, C., Tong, S., Xue, C., Zhao, X., Ge, M., and Mu, Y.: Atmospheric NO_x oxidation as major sources for nitrous acid (HONO), *NPJ Clim. Atmos. Sci.*, 6, doi: 10.1038/s41612-023-00357-8, 2023.
- Spataro, F., Ianniello, A., Esposito, G., Allegrini, I., Zhu, T., and Hu, M.: Occurrence of atmospheric nitrous acid in the urban area of Beijing (China), *Sci. Total Environ.*, 447, 210–224, doi: 10.1016/j.scitotenv.2012.12.065, 2013.
- 605 Stutz, J., B. Alicke, and A. Neftel, Nitrous acid formation in the urban atmosphere: Gradient measurements of NO₂ and HONO over grass in Milan, Italy. *Journal of Geophysical Research-Atmospheres*, 2002. 107(D22).
- Stolzenburg, D., Cai, R., Blichner, S. M., Kontkanen, J., Zhou, P., Makkonen, R., Kerminen, V.-M., Kulmala, M., Riipinen, I., and Kangasluoma, J.: Atmospheric nanoparticle growth, *Rev. Mod. Phys.*, 95, 045002, doi: 10.1103/RevModPhys.95.045002, 2023.
- 610 Su, H., Cheng, Y. F., Shao, M., Gao, D. F., Yu, Z. Y., Zeng, L. M., Slanina, J., Zhang, Y. H., and Wiedensohler, A.: Nitrous acid (HONO) and its daytime sources at a rural site during the 2004 PRIDE - PRD experiment in China, *J. Geophys. Res. Atmos.*, 113, doi: 10.1029/2007jd009060, 2008.
- Su, H., Cheng, Y., Oswald, R., Behrendt, T., Trebs, I., Meixner, F. X., Andreae, M. O., Cheng, P., Zhang, Y., and Pöschl, U.: Soil nitrite as a source of atmospheric HONO and OH radical, *Science*, 333, 1616–1618, doi: 10.1126/science.1207687, 2011.
- 615 Tan, Z., Fuchs, H., Lu, K., Hofzumahaus, A., Bohn, B., Broch, S., Dong, H., Gomm, S., Häsel, R., He, L., Holland, F., Li, X., Liu, Y., Lu, S., Rohrer, F., Shao, M., Wang, B., Wang, M., Wu, Y., Zeng, L., Zhang, Y., Wahner, A., and Zhang, Y.: Radical chemistry at a rural site (Wangdu) in the North China Plain: observation and model calculations of OH, HO₂ and RO₂ radicals, *Atmos. Chem. Phys.*, 17, 663–690, <https://doi.org/10.5194/acp-17-663-2017>, 2017.
- 620 Tan, Z., Rohrer, F., Lu, K., Ma, X., Bohn, B., Broch, S., Dong, H., Fuchs, H., Gkatzelis, G. I., Hofzumahaus, A., Holland, F., Li, X., Liu, Y., Liu, Y., Novelli, A., Shao, M., Wang, H., Wu, Y., Zeng, L., Hu, M., Kiendler-Scharr, A., Wahner, A., and Zhang, Y.: Wintertime photochemistry in Beijing: observations of RO_x radical concentrations in the North China Plain during the BEST-ONE campaign, *Atmos. Chem. Phys.*, 18, 12391–12411, <https://doi.org/10.5194/acp-18-12391-2018>, 2018.
- 625 Tong, S., Hou, S., Zhang, Y., Chu, B., Liu, Y., He, H., Zhao, P., and Ge, M.: Comparisons of measured nitrous acid (HONO) concentrations in a pollution period at urban and suburban Beijing, in autumn of 2014, *Sci China Chem*, 58, 1393–1402, doi: 10.1007/s11426-015-5454-2, 2015.
- VandenBoer, T.C., S.S. Brown, J.G. Murphy, W.C. Keene, C.J. Young, A.A.P. Pszenny, S. Kim, C. Warneke, J. de Gouw, J.R. Maben, N.L. Wagner, T.P. Riedel, J.A. Thornton, D.E. Wolfe, W.P. Dubé, F. Öztürk, C.A. Brock, N. Grossberg, B. Lefer, 630 B.M. Lerner, A.M. Middlebrook, and J.M. Roberts, Understanding the role of the ground surface in HONO vertical structure: High resolution vertical profiles during NACHTT-11. *J. Geophys. Res.*, 2013. 118(17): p. 10155-10171.
- VandenBoer, T. C., Young, C. J., Talukdar, R. K., Markovic, M. Z., Brown, S. S., Roberts, J. M., and Murphy, J. G.: Nocturnal loss and daytime source of nitrous acid through reactive uptake and displacement, *Nat. Geosci.*, 8, 55-60, 10.1038/ngeo2298, 2015.
- 635 Veres, P. R., Roberts, J. M., Wild, R. J., Edwards, P. M., Brown, S. S., Bates, T. S., Quinn, P. K., Johnson, J. E., Zamora, R. J., and de Gouw, J.: Peroxynitric acid (HO₂NO₂) measurements during the UBWOS 2013 and 2014 studies using iodide ion chemical ionization mass spectrometry, *Atmospheric Chemistry and Physics*, 15, 8101-8114, 10.5194/acp-15-8101-2015, 2015.
- Wang, J., Zhang, X., Guo, J., Wang, Z., and Zhang, M.: Observation of nitrous acid (HONO) in Beijing, China: Seasonal variation, nocturnal formation and daytime budget, *Sci. Total Environ.*, 587–588, 350–359, doi: 10.1016/j.scitotenv.2017.02.159, 2017a.
- 640 Wang, J., Gao, J., Che, F., Yang, X., Yang, Y., Liu, L., Xiang, Y., and Li, H.: Summertime response of ozone and fine particulate matter to mixing layer meteorology over the North China Plain, *Atmos. Chem. Phys.*, 23, 14715–14733, doi:

- 10.5194/acp-23-14715-2023, 2023a.
- 645 Wang, J. Q., Gao, J., Che, F., Wang, Y. L., Lin, P. C., and Zhang, Y. C.: Dramatic changes in aerosol composition during the 2016-2020 heating seasons in Beijing-Tianjin-Hebei region and its surrounding areas: The role of primary pollutants and secondary aerosol formation, *Sci. Total Environ.*, 849, 157621, doi: 10.1016/j.scitotenv.2022.157621, 2022.
- Wang, S., R. Ackermann, and J. Stutz, Vertical profiles of NO_x chemistry in the polluted nocturnal boundary layer in Phoenix, AZ: I. Field observations by long-path DOAS. *Atmos. Chem. Phys.*, 2006. 6: p. 2671-2693.
- 650 Wang, T., Xue, L., Brimblecombe, P., Lam, Y. F., Li, L., and Zhang, L.: Ozone pollution in China: A review of concentrations, meteorological influences, chemical precursors, and effects, *Sci. Total Environ.*, 575, 1582–1596, doi: 10.1016/j.scitotenv.2016.10.081, 2017b.
- Wang, Y., Wang, J., Wang, Y., Zhang, Y., Woodward-Massey, R., Zhang, C., Kuang, Y., Zhu, J., Shang, J., Li, X., Zeng, L., Lin, W., and Ye, C.: Experimental and kinetic model evaluation of HONO production from surface nitrate photolysis, *Atmos. Environ.*, 296, 119568, doi: 10.1016/j.atmosenv.2022.119568, 2023b.
- 655 Weber, B., Wu, D., Tamm, A., Ruckteschler, N., Rodríguez-Caballero, E., Steinkamp, J., Meusel, H., Elbert, W., Behrendt, T., Sörgel, M., Cheng, Y., Crutzen, P. J., Su, H., and Pöschl, U.: Biological soil crusts accelerate the nitrogen cycle through large NO and HONO emissions in drylands, *Proc. Natl. Acad. Sci. U.S.A.*, 112, 15384–15389, doi: 10.1073/pnas.1515818112, 2015.
- 660 Wingen, L. M., Moskun, A. C., Johnson, S. N., Thomas, J. L., Roeselova, M., Tobias, D. J., Kleinman, M. T., and Finlayson-Pitts, B. J.: Enhanced surface photochemistry in chloride-nitrate ion mixtures, *Physical chemistry chemical physics: Phys. Chem. Chem. Phys.*, 10, 5668–5677, doi: 10.1039/b806613b, 2008.
- Wong, K. W., Oh, H. J., Lefter, B. L., Rappenglück, B., and Stutz, J.: Vertical profiles of nitrous acid in the nocturnal urban atmosphere of Houston, TX, *Atmospheric Chemistry and Physics*, 11, 3595-3609, 10.5194/acp-11-3595-2011, 2011.
- 665 Wong, K. W., Tsai, C., Lefter, B., Haman, C., Grossberg, N., Brune, W. H., Ren, X., Luke, W., and Stutz, J.: Daytime HONO vertical gradients during SHARP 2009 in Houston, TX, *Atmospheric Chemistry and Physics*, 12, 635-652, 10.5194/acp-12-635-2012, 2012.
- Wong, K. W., Tsai, C., Lefter, B., Grossberg, N., and Stutz, J.: Modeling of daytime HONO vertical gradients during SHARP 2009, *Atmospheric Chemistry and Physics*, 13, 3587-3601, 10.5194/acp-13-3587-2013, 2013.
- 670 Wu, D., Horn, M. A., Behrendt, T., Muller, S., Li, J., Cole, J. A., Xie, B., Ju, X., Li, G., Ermel, M., Oswald, R., Frohlich-Nowoisky, J., Hoor, P., Hu, C., Liu, M., Andreae, M. O., Pöschl, U., Cheng, Y., Su, H., Trebs, I., Weber, B., and Sörgel, M.: Soil HONO emissions at high moisture content are driven by microbial nitrate reduction to nitrite: Tackling the HONO puzzle, *ISME J*, 13, 1688–1699, doi: 10.1038/s41396-019-0379-y, 2019.
- Wu, Z., Hu, M., Shao, K., and Slanina, J.: Acidic gases, NH₃ and secondary inorganic ions in PM₁₀ during summertime in Beijing, China and their relation to air mass history, *Chemosphere*, 76, 1028–1035, doi: 10.1016/j.chemosphere.2009.04.066, 2009.
- 675 Xinghua, L., Shuxiao, W., Lei, D., Jiming, H., Chao, L., Yaosheng, C., and Yang, L.: Particulate and trace gas emissions from open burning of wheat straw and corn stover in China, *Environ. Sci. Technol.*, 41, 6052–6058, doi: 10.1021/es0705137, 2007.
- 680 Xu, W., Kuang, Y., Zhao, C., Tao, J., Zhao, G., Bian, Y., Yang, W., Yu, Y., Shen, C., Liang, L., Zhang, G., Lin, W., and Xu, X.: NH₃-promoted hydrolysis of NO₂ induces explosive growth in HONO, *Atmos. Chem. Phys.*, 19, 10557–10570, doi: 10.5194/acp-19-10557-2019, 2019.
- Xu, Z., Wang, T., Wu, J. Q., Xue, L. K., Chan, J., Zha, Q. Z., Zhou, S. Z., Louie, P. K. K., and Luk, C. W. Y.: Nitrous acid (HONO) in a polluted subtropical atmosphere: Seasonal variability, direct vehicle emissions and heterogeneous production at ground surface, *Atmos. Environ.*, 106, 100–109, doi: 10.1016/j.atmosenv.2015.01.061, 2015.
- 685 Xuan, H., Zhao, Y., Ma, Q., Chen, T., Liu, J., Wang, Y., Liu, C., Wang, Y., Liu, Y., Mu, Y., and He, H.: Formation mechanisms and atmospheric implications of summertime nitrous acid (HONO) during clean, ozone pollution and double high-level PM_{2.5} and O₃ pollution periods in Beijing, *Sci. Total Environ.*, 857, 159538, doi: 10.1016/j.scitotenv.2022.159538, 2023.
- 690 Xue, C., Ye, C., Zhang, C., Catoire, V., Liu, P., Gu, R., Zhang, J., Ma, Z., Zhao, X., Zhang, W., Ren, Y., Krysztofiak, G., Tong, S., Xue, L., An, J., Ge, M., Mellouki, A., and Mu, Y.: Evidence for strong HONO emission from fertilized agricultural fields and its remarkable impact on regional O₃ pollution in the summer North China Plain, *ACS Earth Space Chem.*, 5, 340–347, doi: 10.1021/acsearthspacechem.0c00314, 2021.

- 695 Xue, C., Zhang, C., Ye, C., Liu, P., Catoire, V., Krysztofiak, G., Chen, H., Ren, Y., Zhao, X., Wang, J., Zhang, F., Zhang, C., Zhang, J., An, J., Wang, T., Chen, J., Kleffmann, J., Mellouki, A., and Mu, Y.: HONO Budget and Its Role in Nitrate Formation in the Rural North China Plain, *Environmental Science & Technology*, 54, 11048–11057, 10.1021/acs.est.0c01832, 2020.
- Yang, W., Han, C., Yang, H., and Xue, X.: Significant HONO formation by the photolysis of nitrates in the presence of humic acids, *Environ. Pollut.*, 243, 679–686, doi: 10.1016/j.envpol.2018.09.039, 2018.
- 700 Yang, W., Han, C., Zhang, T., Tang, N., Yang, H., and Xue, X.: Heterogeneous photochemical uptake of NO₂ on the soil surface as an important ground-level HONO source, *Environ. Pollut.*, 271, 116289, doi: 10.1016/j.envpol.2020.116289, 2021a.
- 705 Yang, X., Lu, K., Ma, X., Liu, Y., Wang, H., Hu, R., Li, X., Lou, S., Chen, S., Dong, H., Wang, F., Wang, Y., Zhang, G., Li, S., Yang, S., Yang, Y., Kuang, C., Tan, Z., Chen, X., Qiu, P., Zeng, L., Xie, P., and Zhang, Y.: Observations and modeling of OH and HO₂ radicals in Chengdu, China in summer 2019, *Sci. Total Environ.*, 772, 144829, doi: 10.1016/j.scitotenv.2020.144829, 2021b.
- Ye, C., Zhang, N., Gao, H., and Zhou, X.: Matrix effect on surface-catalyzed photolysis of nitric acid, *Sci. Rep.*, 9, 4351, doi: 10.1038/s41598-018-37973-x, 2019.
- 710 Ye, C. X., Zhang, N., Gao, H. L., and Zhou, X. L.: Photolysis of particulate nitrate as a source of HONO and NO_x, *Environ. Sci. Technol.*, 51, 6849–6856, doi: 10.1021/acs.est.7b00387, 2017.
- Young, C.J., R.A. Washenfelder, L.H. Mielke, H.D. Osthoff, P. Veres, A.K. Cochran, T.C. VandenBoer, H. Stark, J. Flynn, N. Grossberg, C.L. Haman, B. Lefer, J.B. Gilman, W.C. Kuster, C. Tsai, O. Pikelnaya, J. Stutz, J.M. Roberts, and S.S. Brown, Vertically resolved measurements of nighttime radical reservoirs in Los Angeles and their contribution to the urban radical budget. *Environ. Sci. Technol.*, 2012. 46: p. 10965-10973.
- 715 Yu, C. A., Huang, L. B., Xue, L. K., Shen, H. Q., Li, Z. Y., Zhao, M., Yang, J., Zhang, Y. N., Li, H. Y., Mu, J. S., and Wang, W. X.: Photoenhanced heterogeneous uptake of NO₂ and HONO formation on authentic winter time urban grime, *ACS Earth Space Chem.*, 6, 1960–1968, doi: 10.1021/acsearthspacechem.2c00054, 2022a.
- 720 Yu, Y., Cheng, P., Li, H., Yang, W., Han, B., Song, W., Hu, W., Wang, X., Yuan, B., Shao, M., Huang, Z., Li, Z., Zheng, J., Wang, H., and Yu, X.: Budget of nitrous acid (HONO) at an urban site in the fall season of Guangzhou, China, *Atmos. Chem. Phys.*, 22, 8951–8971, doi: 10.5194/acp-22-8951-2022, 2022b.
- Yun, H., Wang, Z., Zha, Q., Wang, W., Xue, L., Zhang, L., Li, Q., Cui, L., Lee, S., Poon, S. C. N., and Wang, T.: Nitrous acid in a street canyon environment: Sources and contributions to local oxidation capacity, *Atmos. Environ.*, 167, 223–234, doi: 10.1016/j.atmosenv.2017.08.018, 2017.
- 725 Zhang, J., Chen, J., Xue, C., Chen, H., Zhang, Q., Liu, X., Mu, Y., Guo, Y., Wang, D., Chen, Y., Li, J., Qu, Y., and An, J.: Impacts of six potential HONO sources on HO_x budgets and SOA formation during a wintertime heavy haze period in the North China Plain, *Sci. Total Environ.*, 681, 110–123, doi: 10.1016/j.scitotenv.2019.05.100, 2019a.
- Zhang, J., Lian, C., Wang, W., Ge, M., Guo, Y., Ran, H., Zhang, Y., Zheng, F., Fan, X., Yan, C., Daellenbach, K. R., Liu, Y., Kulmala, M., and An, J.: Amplified role of potential HONO sources in O₃ formation in North China Plain during autumn haze aggravating processes, *Atmos. Chem. Phys.*, 22, 3275–3302, doi: 10.5194/acp-22-3275-2022, 2022.
- 730 Zhang, Q., Liu, P., Wang, Y., George, C., Chen, T., Ma, S., Ren, Y., Mu, Y., Song, M., Herrmann, H., Mellouki, A., Chen, J., Yue, Y., Zhao, X., Wang, S., and Zeng, Y.: Unveiling the underestimated direct emissions of nitrous acid (HONO), *Proc. Natl. Acad. Sci. U.S.A.*, 120, e2302048120, doi: 10.1073/pnas.2302048120, 2023a.
- Zhang, R. F., Gen, M. S., Huang, D. D., Li, Y. J., and Chan, C. K.: Enhanced sulfate production by nitrate photolysis in the presence of halide ions in atmospheric particles, *Environ. Sci. Technol.*, 54, 3831–3839, doi: 10.1021/acs.est.9b06445, 2020.
- 735 Zhang, W., Tong, S., Ge, M., An, J., Shi, Z., Hou, S., Xia, K., Qu, Y., Zhang, H., Chu, B., Sun, Y., and He, H.: Variations and sources of nitrous acid (HONO) during a severe pollution episode in Beijing in winter 2016, *Sci. Total Environ.*, 648, 253–262, doi: 10.1016/j.scitotenv.2018.08.133, 2019b.
- 740 Zhang, W., Tong, S., Lin, D., Li, F., Zhang, X., Wang, L., Ji, D., Tang, G., Liu, Z., Hu, B., and Ge, M.: Atmospheric chemistry of nitrous acid and its effects on hydroxyl radical and ozone at the urban area of Beijing in early spring 2021, *Environ. Pollut.*, 316, 120710, doi: 10.1016/j.envpol.2022.120710, 2023b.
- Zhang, X., Li, H., Wang, X., Zhang, Y., Bi, F., Wu, Z., Liu, Y., Zhang, H., Gao, R., Xue, L., Zhang, Q., Chen, Y., Chai, F., and Wang, W.: Heavy ozone pollution episodes in urban Beijing during the early summertime from 2014 to 2017:

- Implications for control strategy, *Environ. Pollut.*, 285, 117162, doi: 10.1016/j.envpol.2021.117162, 2021a.
- 745 Zhang, X., Tong, S., Jia, C., Zhang, W., Wang, Z., Tang, G., Hu, B., Liu, Z., Wang, L., Zhao, P., Pan, Y., and Ge, M.: Elucidating HONO formation mechanism and its essential contribution to OH during haze events, *NPJ Clim. Atmos. Sci.*, 6, doi: 10.1038/s41612-023-00371-w, 2023c.
- Zhang, Y., Shindell, D., Seltzer, K., Shen, L., Lamarque, J.-F., Zhang, Q., Zheng, B., Xing, J., Jiang, Z., and Zhang, L.: Impacts of emission changes in China from 2010 to 2017 on domestic and intercontinental air quality and health effect, *Atmos. Chem. Phys.*, 21, 16051–16065, doi: 10.5194/acp-21-16051-2021, 2021b.
- 750 Zhong, X., Shen, H., Zhao, M., Zhang, J., Sun, Y., Liu, Y., Zhang, Y., Shan, Y., Li, H., Mu, J., Yang, Y., Nie, Y., Tang, J., Dong, C., Wang, X., Zhu, Y., Guo, M., Wang, W., and Xue, L.: Nitrous acid budgets in the coastal atmosphere: potential daytime marine sources, *Atmos. Chem. Phys.*, 23, 14761–14778, doi: 10.5194/acp-23-14761-2023, 2023.
- 755 Zhu, T., Tang, M., Gao, M., Bi, X., Cao, J., Che, H., Chen, J., Ding, A., Fu, P., Gao, J., Gao, Y., Ge, M., Ge, X., Han, Z., He, H., Huang, R.-J., Huang, X., Liao, H., Liu, C., Liu, H., Liu, J., Liu, S. C., Lu, K., Ma, Q., Nie, W., Shao, M., Song, Y., Sun, Y., Tang, X., Wang, T., Wang, T., Wang, W., Wang, X., Wang, Z., Yin, Y., Zhang, Q., Zhang, W., Zhang, Y., Zhang, Y., Zhao, Y., Zheng, M., Zhu, B., and Zhu, J.: Recent progress in atmospheric chemistry research in China: Establishing a theoretical framework for the “Air pollution complex”, *Adv. Atmos. Sci.*, 40, 1339–1361, doi: 10.1007/s00376-023-2379-0, 2023.
- 760